

Journal of
Cognitive Neuroscience**Rhythmic temporal cues coordinate cross-frequency phase-amplitude coupling during memory encoding**

Journal:	<i>Journal of Cognitive Neuroscience</i>
Manuscript ID	Draft
Manuscript Type:	Original
Date Submitted by the Author:	n/a
Complete List of Authors:	Hickey Townsend, Paige; Massachusetts General Hospital, Psychiatry; Athinoula A Martinos Center for Biomedical Imaging Jones, Alexander; Middlesex University - Hendon Campus, Psychology Patel, Aniruddh; Tufts University, Psychology; Canadian Institute for Advanced Research, Program in Brain, Mind, and Consciousness Race, Elizabeth; Tufts University, Psychology
Keywords:	Rhythm, Entrainment, Oscillations, Music, Episodic Memory

SCHOLARONE™
Manuscripts

1
2
3
4
5
6
7
8 **Rhythmic temporal cues coordinate cross-frequency phase-amplitude coupling during**
9 **memory encoding**
10

11
12 Paige Hickey Townsend^{a,b}, Alexander Jones^c, Aniruddh D. Patel^{d,e} and Elizabeth Race^d
13

14 ^aDepartment of Psychiatry and Pediatrics, Massachusetts General Hospital, Harvard Medical
15 School, Boston, MA, USA

16 ^bAthinoula A. Martinos Center for Biomedical Imaging, Charlestown, MA, USA

17 ^cMiddlesex University, Hendon, London NW4 4BT

18 ^dTufts University, Medford, MA 02155

19 ^eProgram in Brain, Mind, and Consciousness, Canadian Institute for Advanced Research
20 (CIFAR), Toronto, ON M5G1M1
21
22

23
24
25 **Conflict of Interest**

26 The authors declare no competing financial interests.
27

28 **Acknowledgements**

29 This research was funded (in part) by a grant from the GRAMMY Museum®.
30
31
32
33
34
35
36
37
38
39
40
41
42
43
44
45
46
47
48
49
50
51
52
53
54
55
56
57
58
59
60

Abstract

Accumulating evidence suggests that rhythmic temporal cues in the environment influence the encoding of information into long-term memory. Here, we test the hypothesis that these mnemonic effects of rhythm reflect the coupling of high-frequency (gamma) oscillations to entrained lower-frequency oscillations synchronized to the beat of the rhythm. In Study 1, we first test this hypothesis in the context of global effects of rhythm on memory, when memory is superior for visual stimuli presented in rhythmic compared to arrhythmic patterns at encoding (Jones & Ward, 2019). We found that the mnemonic benefit of rhythm was associated with increased phase-amplitude coupling (PAC) between entrained low-frequency (delta) oscillations and higher-frequency (gamma) oscillations. In Study 2, we next investigated cross-frequency PAC in the context of local effects of auditory rhythm on memory encoding, in which subsequent memory is superior for information presented in-synchrony compared to out-of-synchrony with a background beat (Hickey et al., 2020). We found that the mnemonic benefit of rhythm in this context was also associated with increased cross-frequency PAC between entrained low-frequency (delta) oscillations and higher-frequency (gamma) oscillations, and that the magnitude of gamma power modulations scaled with the subsequent memory benefit for in-versus out-of-synchrony stimuli. Together, these results suggest that it is not entrained low-frequency oscillations themselves that modulate memory encoding, but the coordination of higher-frequency gamma activity by entrained low-frequency oscillations.

Keywords: Rhythm, Entrainment, Oscillations, Music, Episodic Memory

Introduction

Rhythmically-structured sounds such as speech or music contain predictable temporal patterns, and a large body of work has demonstrated that the brain can leverage such patterns to optimize perception and action (Jones, 2019; Jones & Boltz, 1989; Large & Jones, 1999). For example, target detection and perceptual discrimination are faster and more accurate when stimuli appear in-synchrony compared to out-of-synchrony with a rhythmic beat (Barnhart et al., 2018; Bolger et al., 2013; Escoffier et al., 2010; Jones et al., 2002). Recently, these dynamic effects of rhythm have been extended to higher-level cognitive processes such as memory. For example, stimuli presented rhythmically at encoding (i.e., with a consistent interstimulus interval) are better remembered in subsequent tests of long-term memory compared to stimuli presented arrhythmically at encoding (i.e., with a variable interstimulus interval; Jones et al., 2022; Jones & Ward, 2019; Thavabalasingam et al., 2015; but see Kulkarni & Hannula, 2021). In addition, the timing of stimulus presentation *within* a rhythmic temporal stream also influences memory encoding, evident in superior subsequent memory for visual stimuli presented synchronously compared to asynchronously with a background beat (Hickey, Merseal, et al., 2020; Johndro et al., 2019). Together, these results suggest that rhythm dynamically modulates memory formation at both the global and local levels. An important outstanding question is how these mnemonic effects of rhythm are instantiated in the brain.

Prior work in the perceptual domain has suggested that the effects of rhythm on behavior result from the synchronization of neural oscillations to the timing of external rhythms (i.e., neural entrainment; Schroeder & Lakatos, 2009). For naturalistic rhythms, such as biological motion, speech, and music which contain salient slow modulations (<5Hz, see Ding et al., 2017; Shen et al., 2023), this synchronization manifests as greater power or phase coherence in lower-

1
2
3 frequency oscillations in the delta range (1-4Hz, see Ding & Simon, 2014; Nozaradan et al.,
4
5 2016; Shen et al., 2023). Low-frequency delta oscillations are known to modulate neural
6
7 excitability across time in a periodic fashion. In the context of rhythm, the phase of these
8
9 oscillations shifts such that windows of heightened neural excitability occur at predictable
10
11 moments (in synchrony with the beat). This alignment of internal and external rhythms has two
12
13 primary effects on the brain and behavior. First, it allows the brain to conserve computational
14
15 resources at the global level by shifting from a more metabolically demanding “vigilance mode”
16
17 of processing to a more efficient “rhythmic mode” of processing (Schroeder & Lakatos, 2009).
18
19 Additionally, low-frequency oscillatory entrainment optimizes the processing of relevant events
20
21 in the environment by creating distinct temporal windows of heightened neural excitability
22
23 optimized for sensory-perceptual processing (rhythmic perceptual sampling; Arnal & Giraud,
24
25 2012; Calderone et al., 2014; Lakatos et al., 2008; Schroeder & Lakatos, 2009). In this way,
26
27 neural entrainment can have more sustained effects on information processing at the global level
28
29 as well as more discrete effects on information processing at the local level.
30
31
32
33
34

35
36 Recent evidence suggests that similar entrainment mechanisms may also underlie the
37
38 effects of rhythm on memory encoding. In a study by Jones and Ward (2019), participants
39
40 incidentally encoded visual images that were either displayed rhythmically every 600ms (1.67
41
42 Hz) or arrhythmically (variable interstimulus interval). Stimuli that were presented rhythmically
43
44 at encoding were better remembered in subsequent tests of memory compared to stimuli
45
46 presented arrhythmically at encoding. Rhythmic stimulus presentation at encoding was also
47
48 associated with oscillatory entrainment, evident in stronger inter-trial phase coherence (ITPC) at
49
50 the same frequency as stimulus presentation (1.67 Hz). While a correlation between the
51
52 magnitude of oscillatory entrainment and memory performance was not observed across
53
54
55
56
57
58
59
60

1
2
3 participants, this suggests that global effects of rhythm on memory encoding may reflect the
4
5 rhythmic coordination of neural oscillations.
6

7
8 Recently, Hickey et al. (2020) found additional evidence linking entrained, low-
9
10 frequency oscillations to the effects of rhythm on memory performance, this time at the local
11
12 level. In this study, participants encoded visual images in the context of background, musical
13
14 rhythm with a steady 1.25 Hz beat, and the timing of image presentation within this rhythmic
15
16 context was manipulated such that stimuli either appeared in-synchrony or out-of-synchrony
17
18 with the beat. At the behavioral level, participants demonstrated superior subsequent memory
19
20 performance for stimuli presented on-beat versus off-beat at encoding. Significant neural
21
22 tracking of the beat was also observed, evident in enhanced inter-trial phase coherence and
23
24 steady state evoked potentials (SSEPs) at the beat frequency (1.25 Hz). Importantly, a strong
25
26 positive association was found between the strength of neural entrainment at the beat frequency
27
28 (1.25 Hz) and the mnemonic effects of rhythm. In addition, at the time of stimulus presentation,
29
30 neural entrainment at the beat frequency was greater for images that were remembered compared
31
32 to those that were forgotten on subsequent tests of memory. Together, these results suggest that
33
34 entrained low-frequency oscillations dynamically modulate memory formation and enhance
35
36 encoding at specific moments in time.
37
38
39
40
41

42 While the aforementioned results support the proposal that entrained low-frequency
43
44 oscillations influence the temporal dynamics of memory encoding at both the global and local
45
46 levels, an important outstanding question is the underlying mechanism by which this occurs. One
47
48 possibility is that effects of rhythm on memory reflect entrained oscillations themselves, and it is
49
50 the modulation of neural activity in sensory cortices which influences local excitability and
51
52 processing efficiency in a rhythmic manner (e.g., ‘sensory gating’) (Lakatos et al., 2008;
53
54
55
56
57
58
59
60

1
2
3 O'Connell et al., 2015; Schroeder & Lakatos, 2009). Alternatively, mnemonic effects of rhythm
4 could reflect the orchestration of higher-frequency oscillatory activity in networks of brain
5 regions beyond the sensory cortices. Indeed, external rhythms have been shown to influence
6 neural activity in widespread brain regions (Besle et al., 2011) and rhythmic stimulation in one
7 modality (e.g., auditory) can influence behavioral performance and neural activity in a different
8 modality (e.g., visual; Hickey et al., 2020; Lakatos et al., 2008). In addition, entrained low-
9 frequency oscillations have been shown to modulate the power of higher-frequency oscillations
10 outside of sensory cortices, such as the parietal and frontal cortices (Keitel et al., 2017), which
11 may be particularly relevant to higher-order cognitive functions such as memory formation.
12 Further support for this proposal comes from an event-related potential study by Hickey, Barnett-
13 Young, et al. (2020), which found that the mnemonic effects of rhythm are related to
14 electrophysiological responses relatively late in the information processing stream (post-
15 perceptual N2 and P3 components). In this way, low-frequency oscillations entrained to external
16 rhythmic cues could dynamically organize activity in multiple frequency bands and brain regions
17 to influence higher-order cognitive processing.

18
19 Here, we explore the proposal that entrained low-frequency oscillations influence
20 memory performance by imposing temporal structure on higher-frequency (gamma) oscillations
21 that are more commonly associated with memory encoding (Hickey & Race, 2021; A. Jones &
22 Ward, 2019). Central to this proposal is the phenomenon of cross-frequency phase-amplitude
23 coupling (PAC), whereby the amplitudes of faster (higher frequency) rhythms, such as gamma
24 oscillations, couple to the phase of slower (lower-frequency) rhythms entrained to environmental
25 stimuli (Buzsáki, 2006; Canolty & Knight, 2010; Lakatos et al., 2005, 2008; Sadeh, 2014).

26 Gamma oscillations occur across a broad range of frequencies (30-100 Hz) and are thought to
27
28
29
30
31
32
33
34
35
36
37
38
39
40
41
42
43
44
45
46
47
48
49
50
51
52
53
54
55
56
57
58
59
60

1
2
3 reflect local processing within cortical regions (Buzsáki & Wang, 2012; Canolty & Knight,
4 2010). Activity in the higher range of gamma (65-100 Hz) has been more commonly associated
5 with memory encoding (Colgin et al., 2009; Griffiths et al., 2019), whereas low-gamma activity
6 has been associated with response speeds on perceptual tasks. Importantly, in addition to
7 influencing sensory and perceptual processing (Bartoli et al., 2019), gamma oscillations, and the
8 coupling of gamma oscillations to lower-frequency oscillations, are proposed to play a key role
9 in memory formation and subsequent memory performance (Canolty & Knight, 2010; Frieze et
10 al., 2013; Jensen et al., 2007; Köster et al., 2019; Lega et al., 2016; Osipova et al., 2006; Rieder
11 et al., 2011; Sederberg et al., 2003, 2007; Trimper et al., 2017). Thus, entrained low-frequency
12 oscillations in sensory-specific cortices (e.g., auditory cortex for auditory rhythms) may
13 indirectly contribute to memory performance by modulating higher-frequency neural activity in
14 the gamma range.

15
16
17
18
19
20
21
22
23
24
25
26
27
28
29
30
31 Support for this proposal comes from a prior study by (Köster et al., 2019) in which low-
32 frequency (theta) oscillatory activity was entrained via visual flicker during the encoding of
33 visual images into memory. While the strength of participants' entrainment to the visual flicker
34 was positively associated with overall memory performance, it was the *coupling* between
35 entrained oscillations and higher-frequency gamma activity which predicted memory
36 performance on individual trials. Specifically, cross-frequency PAC was greater for images that
37 would be later remembered compared to those that would be later forgotten. These findings
38 support the hypothesis that while entrained low-frequency oscillations put the brain into an
39 "optimal" state for encoding, the effect of rhythm on subsequent memory may be more closely
40 related to the orchestration of higher-frequency gamma oscillations entrained to the pace of
41 entrained oscillations (Köster et al., 2019).
42
43
44
45
46
47
48
49
50
51
52
53
54
55
56
57
58
59
60

1
2
3 The current experiments tested this hypothesis in the context of both global and local
4 effects of rhythm on memory encoding. In Study 1, we re-analyzed the dataset collected by Jones
5 and Ward (2019) to investigate whether cross-frequency PAC between entrained low-frequency
6 oscillations and higher-frequency gamma activity was associated with memory performance at
7 the *global* level. If this is the case, then delta-gamma PAC should be greater during encoding
8 blocks in which visual stimuli are presented rhythmically compared to those in which stimuli are
9 presented arrhythmically. Furthermore, the magnitude of PAC differences between rhythmic and
10 arrhythmic blocks may be related to the magnitude of the mnemonic benefit of rhythm across
11 participants. In Study 2, we re-analyzed the dataset collected by Hickey, Merseal, and colleagues
12 (2020) to investigate whether cross-frequency PAC between entrained low-frequency
13 oscillations and higher-frequency gamma activity is associated with the mnemonic effects of
14 rhythm at the *local* level. If this is the case, then significant PAC should be present during
15 encoding in the presence of background music with a steady beat, and the magnitude of this
16 coupling should scale with the magnitude of the memory benefit for on-beat versus off-beat
17 stimuli. When directly comparing on-beat and off-beat trials, we predicted that gamma power
18 would be greater for on-beat trials compared to off-beat trials, and that stronger gamma power at
19 the stimulus level would be related to a greater mnemonic benefit of rhythm.
20
21
22
23
24
25
26
27
28
29
30
31
32
33
34
35
36
37
38
39
40
41

42 Study 1

43 Method

44
45
46
47 Experimental methods have been reported previously (Jones & Ward, 2019), but are summarized
48 here.
49
50

51 Participants

52
53
54
55
56
57
58
59
60

1
2
3 A total of 24 participants (9 male, 15 female) of an average age of 23.3 years ($SD = 2.4$
4 years) completed the experiment. One participant was excluded from the analysis due to poor
5 attention and performance on the task. Participants were all English speakers, had normal or
6 corrected to normal vision, and were right-handed. Participants were compensated £20 for
7 participation. The study was approved by the Middlesex University research ethics committee
8 and all participants provided informed consent prior to participation.
9
10
11
12
13
14
15

16 **Study Design**

17
18
19 The experimental design is illustrated in Figure 1. Each participant completed six
20 experimental blocks in which they first encoded images and then completed a subsequent
21 memory test. In half of the blocks, images were presented rhythmically during encoding
22 (consistent ISI) and in the other half, images were presented arrhythmically (variable ISI).
23
24 Blocks alternated between rhythmic and arrhythmic presentations at encoding and the order of
25 blocks (rhythmic, arrhythmic) was counterbalanced across participants.
26
27
28
29
30
31
32

33 **Procedure**

34
35 During encoding, participants completed a target detection task in which they were
36 shown a series of 40 images and 120 checkerboards in each block. Participants were instructed to
37 press the spacebar whenever they saw an image of an animal (~10% of trials). Images and
38 checkerboards were always displayed on the screen for 600 ms and were separated by a fixation
39 cross. During rhythmic blocks, the fixation cross duration was set at 600 ms, resulting in a
40 rhythmic presentation of images at a frequency of 1.67 Hz. During arrhythmic blocks, the
41 fixation cross had a variable inter-stimulus interval that was determined by randomly sampling
42 from a uniform distribution between 70-1130 ms, but with an average inter-stimulus interval of
43
44
45
46
47
48
49
50
51
52
53
54
55
56
57
58
59
60

approximately 600 ms across the whole block.

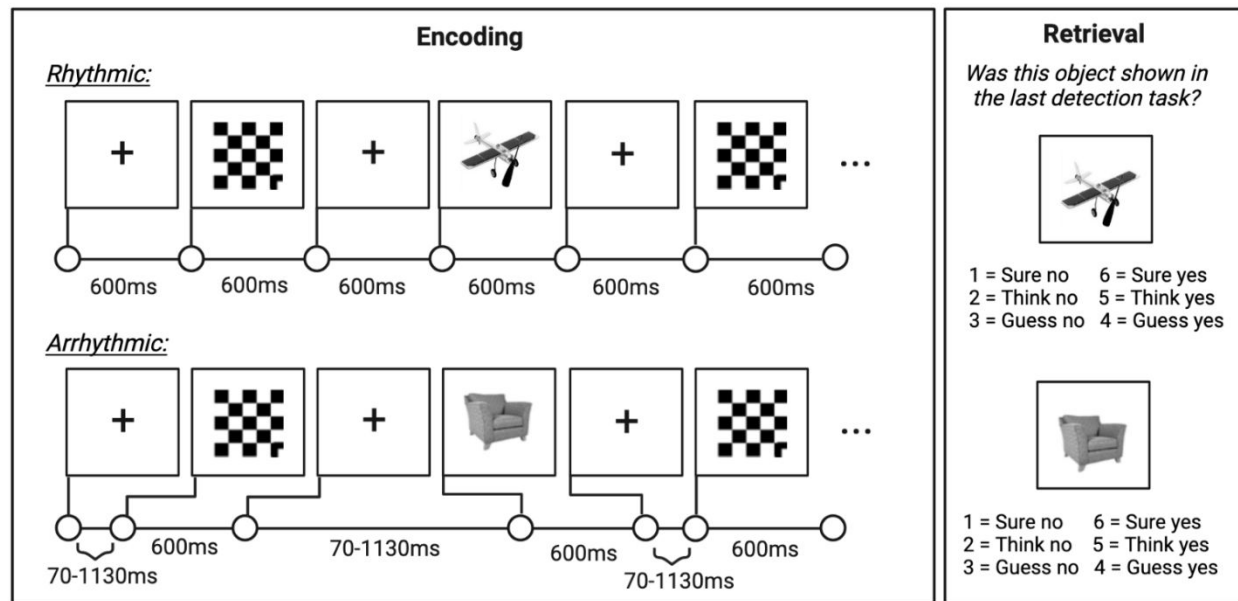


Figure 1. Experimental design for Study 1. Participants completed 6 blocks of encoding and retrieval (3 rhythmic; 3 arrhythmic). During encoding, participants were shown a series of images and checkerboards separated by fixation crosses and instructed to press the space bar each time an animal appeared. Images remained on the screen for 600ms. In rhythmic blocks, the interstimulus interval (ISI) was always 600ms, while in arrhythmic blocks the ISI was jittered between 70-1130ms. Example timelines of stimulus presentation during encoding are illustrated in the first panel. During retrieval, participants were given self-paced memory tests where they were presented with old and new images and indicated if they had seen the image during the preceding detection (encoding) task and their confidence in their memory decision.

After encoding, participants solved simple algorithmic problems for three minutes before they were given a self-paced subsequent memory test where they were shown another series of 80 images (40 images from the detection task and 40 new images). For each image, participants were asked “*Was this object shown in the last detection task?*” and indicated their response with a button press according to a response scale (6 = sure yes, 5 = think yes, 4 = guess yes, 3 = guess no, 2 = think no, 1 = sure no).

Data Analysis

Behavioral Data Analysis

Memory performance from the subsequent memory test was computed separately for each of the rhythmic and arrhythmic blocks. Responses were collapsed across confidence ratings

1
2
3 (1-3 = old items, 4-6 = new items) to determine the proportion of images which were correctly
4 identified as old (hits) and of images incorrectly identified as old (false alarms). From these
5 proportions we calculated using d-prime (d'), a measure of discriminability between previously
6 seen and novel items to mirror the analyses in Experiment 2 and Hickey, Merseal, et al. (2020).
7
8
9

12 ***EEG recording and Preprocessing***

14 EEG was recorded from 64 channels throughout the experiment using a BioSemi Active
15 Two System (BioSemi, Amsterdam, Netherlands). EOG was also recorded to detect eye blinks.
16
17 Preprocessing was completed in the EEGLab toolbox (Delorme & Makeig, 2004) and custom
18
19 MATLAB scripts. First, EEG data was referenced to the average of all electrode channels. EEG
20
21 signals were then downsampled from 2048 Hz (which was the sampling rate the signal was
22
23 recorded with) to 512 Hz and filtered using a 0.1 Hz high pass and 120 Hz low pass filter. After,
24
25 eye artifacts were removed from the signal using independent components analysis. Then, the
26
27 signal was epoched into 6 second windows (Köster et al., 2019), resulting in 10 cycles of the
28
29 low-frequency oscillation per epoch. In total, there were approximately 32 epochs per block.
30
31 Epochs containing muscle artifacts were then removed by visual inspection. Overall, a large
32
33 portion of the epochs were retained in both the rhythmic ($M = 25.35$; $SE = .57$) and the
34
35 arrhythmic conditions ($M = 25.17$; $SE = .57$). The number of epochs did not differ significantly
36
37 based on block number ($F(2,44) = 1.86$, $p = .19$, $\eta^2_p = .08$) or based on rhythmicity ($F(1,22) =$
38
39 $.24$, $p = .63$, $\eta^2_p = .01$).
40
41
42
43
44
45
46

47 ***Phase Amplitude Coupling***

49 Phase-amplitude coupling was calculated between neural oscillations at the rhythmic
50
51 frequency (1.67 Hz) and gamma activity (30-100 Hz) in each block using the PACTools toolbox
52
53 for MATLAB (Martínez-Cancino, 2020). The Modulation Index (MI; Tort et al., 2010) was
54
55
56
57
58
59
60

1.

1
 2
 3 chosen as a measure of PAC based on its use in prior literature (Köster et al., 2019) and its
 4 relative accuracy when compared to other techniques (Hülsemann et al., 2019). The MI was
 5
 6 calculated at electrodes PO7 and PO8. Electrodes PO7 and PO8 were selected given the visual
 7
 8 nature of the entraining stimulus and previous finding by Jones and Ward (2019) of significant
 9
 10 1.67 Hz phase locking (entrainment) at these electrode sites. To calculate the MI, low-frequency
 11
 12 oscillations were filtered between 1-6 Hz in .33 Hz steps, which ensured that phase-amplitude
 13
 14 coupling could be measured at the rhythmic frequency (1.67 Hz), as well as other surrounding
 15
 16 frequencies for comparison. High frequency oscillations were filtered between 30-100 Hz in 5
 17
 18 Hz steps (Köster et al., 2019) before the phase and amplitude time series were obtained using a
 19
 20 Hilbert transform. Gamma amplitudes were sorted according to the corresponding low-frequency
 21
 22 phase (18 bins) and the average gamma amplitude was computed in each low-frequency phase
 23
 24 bin. Next, mean amplitudes were normalized by dividing by the average amplitude across all
 25
 26 phase bins. The Kullback Leibler Distance (DKL) was calculated to determine if the distribution
 27
 28 of the average gamma amplitude across phase bins (P) differs from a uniform distribution (U).
 29
 30 The Kullback Leibler Distance (DKL) can be computed using the following equation, where j
 31
 32 represents each phase bin, N represents the total number of phase bins:

$$DKL(P,U) = \sum_{j=1}^N \left(P(j) \log \left(\frac{P(j)}{U(j)} \right) \right)$$

33
 34
 35 Finally, the MI was calculated by normalizing the DKL (see equation below):
 36
 37

$$MI = \frac{DKL(P,U)}{\log(N)}$$

38
 39
 40 MI values range from 0 – 1, where a value of 0 indicates a completely uniform distribution of
 41
 42 gamma amplitudes by the entrained phase (indicating an absence of phase-amplitude coupling)
 43
 44
 45
 46
 47
 48
 49
 50
 51
 52
 53
 54
 55
 56
 57
 58
 59
 60

1
2
3 and a value of 1 indicates the highest degree of modulation by the entrained phase (strong phase-
4 amplitude coupling).
5
6

7
8 To test for statistical significance, raw MI values (MI_{raw}) were averaged across electrodes
9
10 PO7 and PO8 and were compared to a surrogate distribution (MI_{surr}) (Mariscal et al., 2021). The
11
12 surrogate data was generated in PACTools by randomly shuffling the amplitude time series from
13
14 the original dataset, generating 200 surrogate MI values, and producing a surrogate distribution.
15
16 If significant phase-amplitude coupling occurred, mean MI_{raw} values would be greater than the
17
18 mean of the surrogate values (MI_{surr}). When looking at brain-behavior relationships between
19
20 coupling and subsequent memory performance, MI_{raw} values were standardized (MI_z) using the
21
22 mean and standard deviation of the surrogate sample.
23
24
25

26 MI values were calculated for the low gamma (30-60 Hz) and high gamma (65-100 Hz)
27
28 ranges, following previous studies of memory and phase-amplitude coupling which have
29
30 observed differences in the function of low versus high gamma oscillations, where higher
31
32 frequency gamma activity is more closely tied to memory encoding (Colgin et al., 2009; Griffiths
33
34 et al., 2019; Lega et al., 2016; Tort et al., 2008).
35
36
37

38 **Statistical Analysis Plan**

39
40 All statistics were completed in RStudio. Non-parametric statistics were used to
41
42 determine significance of phase-amplitude coupling because the Modulation Index is on a 0-1
43
44 scale and is therefore non-linear. Analyses using normalized coupling (MI_z) and gamma power
45
46 were completed using parametric statistics, except in cases where distributions were non-
47
48 normally distributed. One participant had outlier MI values ($> 3SD$ above the mean) and was
49
50 excluded from the analysis.
51
52
53
54
55
56
57
58
59
60

To test the hypothesis that coupling between higher-frequency (gamma) oscillations and entrained low-frequency oscillations would occur in the context of rhythm, MI_z values were entered into 2x2x3x2 repeated measures ANOVA containing four within-subjects factors: Gamma Band (high, low), Rhythmicity (rhythmic, arrhythmic), Block (1, 2, 3), and Electrode (PO7, PO8). To evaluate the significance of phase-amplitude coupling in rhythmic and arrhythmic blocks, MI_{raw} and MI_{surr} values were averaged across blocks and electrodes and entered into a Wilcoxon Signed Rank test. Given that the primary analysis of interest was the comparison of rhythmic and arrhythmic contexts, only results involving main effects of rhythmicity are included. Pearson correlations were also used to test whether there was a relationship between PAC and the effect of rhythm on memory. Bayes Factors (BF) were also computed using JASP (Version 0.17.1; JASP Team, 2023) for all null effects including Rhythmicity which were related to our hypotheses of interest.

Results

Figure 2A depicts phase-amplitude coupling between low-frequency oscillations at the beat frequency (1.67 Hz) and higher-frequency gamma oscillations. There was not a significant main effect of Rhythmicity ($F(1,21) = 0.71, p = 0.41, \eta^2_p = 0.03, BF_{10} = .281$) nor Gamma Band ($F(1,21) = 0.03, p = 0.87, \eta^2_p = 0.001, BF_{10} = .155$), but there was a significant interaction between Gamma Band and Rhythmicity ($F(1,21) = 7.60, p = .012, \eta^2_p = .27$), indicating that rhythm had different effects on the magnitude of cross-frequency PAC for oscillations in the low-gamma (30-60 Hz) versus the high-gamma range (65-100 Hz). Indeed, follow-up analysis indicated that coupled oscillations in the low gamma range did not differ between rhythmic and arrhythmic contexts (Figure 2C; $F(1,21) = 2.67, p = .12, BF_{10} = .702$), but that coupled oscillations in the high-gamma range were numerically greater during rhythmic compared to

arrhythmic contexts (Figure 2B; $F(1,21) = 4.02$, $p = .058$, $BF10 = 1.197$). No other significant 2-way, 3-way, or 4-way interactions involving Rhythmicity were found ($F_s < 1.98$, $p_s > .17$, $BF10_s < .132$). Given that there was also no main effect of Block or Electrode ($p_s > .10$, $BF10_s < .479$), subsequent phase-amplitude coupling analyses averaged MI values across blocks and electrodes.

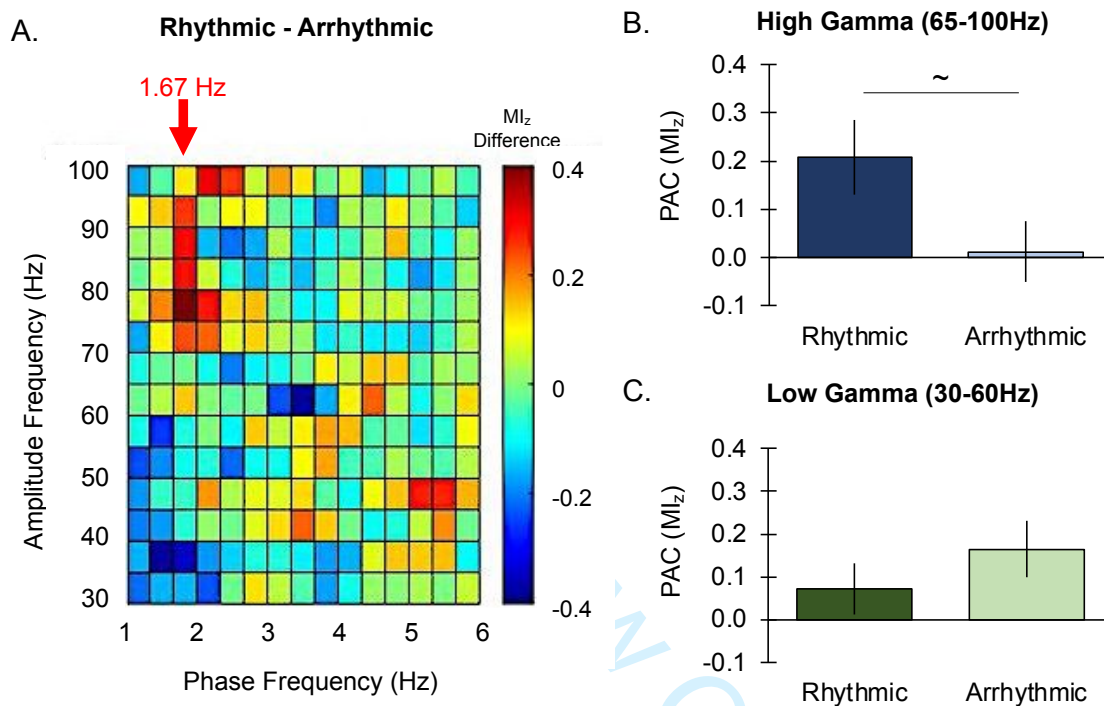


Figure 2. The difference in normalized Phase-Amplitude Coupling (PAC; measured by MI_z) between rhythmic and arrhythmic contexts. (A) The comodulogram depicts the difference in PAC between contexts (rhythmic – arrhythmic), where the third column displays coupling at the entraining frequency (1.67 Hz). (B) There was numerically greater phase-amplitude coupling at the entrained (1.67 Hz) frequency in the high-gamma (65-100 Hz) range, (C) but not in the low-gamma (30-60 Hz) range. Error bars represent SEM. $\sim p = .058$.

To evaluate the significance of phase-amplitude coupling within the rhythmic and arrhythmic blocks individually, raw MI values (MI_{raw}) were compared to a surrogate distribution (MI_{surr}) in each of condition (rhythmic, arrhythmic). In the rhythmic blocks, MI_{raw} values were significantly greater than the surrogate ($Z = -2.23$, $p = .013$, $r = .34$), whereas there was not evidence of significant coupling in the arrhythmic blocks ($Z = -1.19$, $p = .88$, $r = .18$, $BF10 = .235$). These results confirm that coupling between the phase of entrained 1.67 Hz oscillations

and the amplitude of higher-frequency (65-100 Hz) gamma oscillations occurs selectively in the context of rhythm (Figure 3).

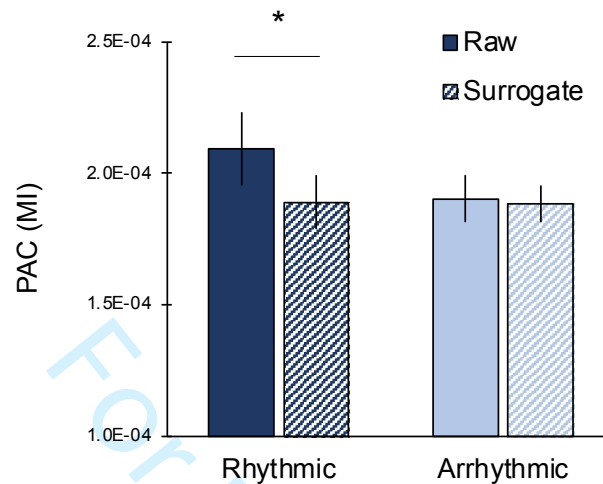
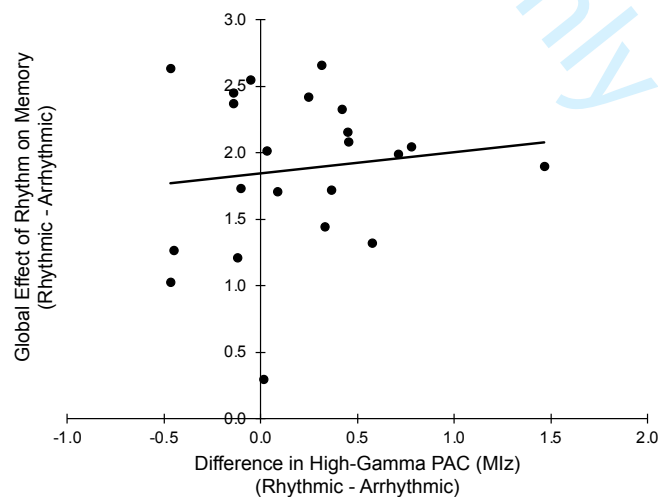


Figure 3. Significant phase-amplitude coupling (PAC; measured by MI) between the phase of entrained (1.67 Hz) oscillations and the amplitude of high-gamma (65-100 Hz) oscillations occurred in the rhythmic context only. Error bars represent SEM. * $p < .05$

Brain-Behavior Relationships

We next investigated if the effects of rhythm on the magnitude of phase-amplitude coupling between oscillations at the beat frequency (1.65 Hz) and oscillations in the high gamma



range (65-100 Hz) was related to the effect of rhythm on memory performance. There was not a significant correlation between these two variables across individuals ($r(20) = .12, p = .59, BF_{10}$

Figure 4. The difference in high-gamma phase amplitude coupling (PAC) between rhythmic and arrhythmic blocks showed a non-significant positive relationship with the global effect of rhythm on memory (d' rhythmic - d' arrhythmic).

1
2
3 = .303). However, the relationship was in the expected direction. One participant showed a large
4
5 difference in high-gamma PAC, but their inclusion did not effect the results ($r(19) = .15, p = .52,$
6
7 $BF10 = .327$).
8
9

10 **Interim Discussion**

11
12 The results from Study 1 reveal that low-frequency oscillations entrained to
13
14 environmental rhythms impose temporal structure on higher-frequency (gamma) oscillations
15
16 during memory encoding through a process of phase-amplitude coupling (PAC). These results
17
18 support the hypothesis that in the context of rhythm, the brain operates in a ‘rhythmic mode’ in
19
20 which gamma oscillations couple to entrained low-frequency oscillations and serve as a
21
22 mechanism of selective attention that can influence both perception and cognition (Canolty &
23
24 Knight, 2010; Köster et al., 2019; Schroeder & Lakatos, 2009). While we did not observe a
25
26 significant relationship between the magnitude of entrained PAC and the global effect of rhythm
27
28 on memory formation across participants, the directionality of the relationship was consistent
29
30 with our predictions: stronger PAC was associated with greater effects of rhythm on memory. In
31
32 Study 2, we turn our attention to the relationship between cross-frequency PAC and the effects of
33
34 rhythm at the local level. Importantly, in contrast to Study 1 where the primary comparison was
35
36 between rhythmic and arrhythmic contexts, in Study 2 stimuli were always presented in the
37
38 context of rhythm but occurred either in-synchrony or out-of-synchrony with the beat. This
39
40 enabled us to investigate the effects of rhythm on PAC at the local level by comparing PAC
41
42 during distinct temporal windows (on-beat vs. off-beat) during the rhythmic temporal stream.
43
44
45
46
47
48

49 **Study 2**

50 **Method**

51
52
53
54
55
56
57
58
59
60

1
2
3 Experimental methods have been reported previously (Hickey, Merseal, et al., 2020), but
4 are summarized here.
5
6

7 **Participants**

8
9
10 A total of 36 individuals (12 male, 24 female) between 18-31 years of age ($M = 23$, $SD =$
11
12 3.32) participated in Study 2. All participants were right-handed, fluent English speakers, and
13
14 had normal or corrected to normal sight and hearing. Additionally, participants did not have a
15
16 history of neurological illness, brain injury, or any psychiatric diagnosis. Participants were
17
18 recruited from the Tufts University community and received either \$15/hour or course credit for
19
20 participation. All participants provided informed consent according to the procedures from the
21
22 Institutional Review Board at Tufts University.
23
24
25

26 **Study Design**

27
28 Participants first encoded images of objects in the context of background music, half of
29
30 which occurred synchronously with beat of the background music (on-beat), and half of which
31
32 occurred 250ms prior to the beat (off-beat). Afterwards, participants completed a self-paced
33
34 subsequent memory test in silence.
35
36
37

38 **Procedure**

39
40 The experimental design of Study 2 is illustrated in Figure 5. During encoding,
41
42 participants viewed a series of visual stimuli in the context of instrumental background music
43
44 with a steady 75 bpm beat (i.e., 1.25 Hz beat rate, inter-beat-interval = 800 ms). The music
45
46 stimulus was developed using GarageBand (Apple Inc.) and was looped throughout the encoding
47
48 task, lasting about 13 minutes (for more details about the musical stimulus, please see Hickey,
49
50 Merseal, et al., 2020). Participants listened to the music through headphones and were informed
51
52 that music would play in the background during the task. The volume of the music was set to a
53
54
55
56
57
58
59
60

comfortable listening level and kept constant across participants. In total, 120 objects were presented (60 living, 60 non-living) in the center of the screen for 750ms with a jittered inter-onset interval (IOI) between images ($M = 6.4s$, $SD = 1.25s$). Participants were instructed to decide whether each depicted a living or non-living object as quickly and accurately as possible. Importantly, images appeared either in-synchrony or out-of- synchrony with the beat of the background music (intermixed throughout the task).

Immediately after encoding, participants were administered a surprise, self-paced

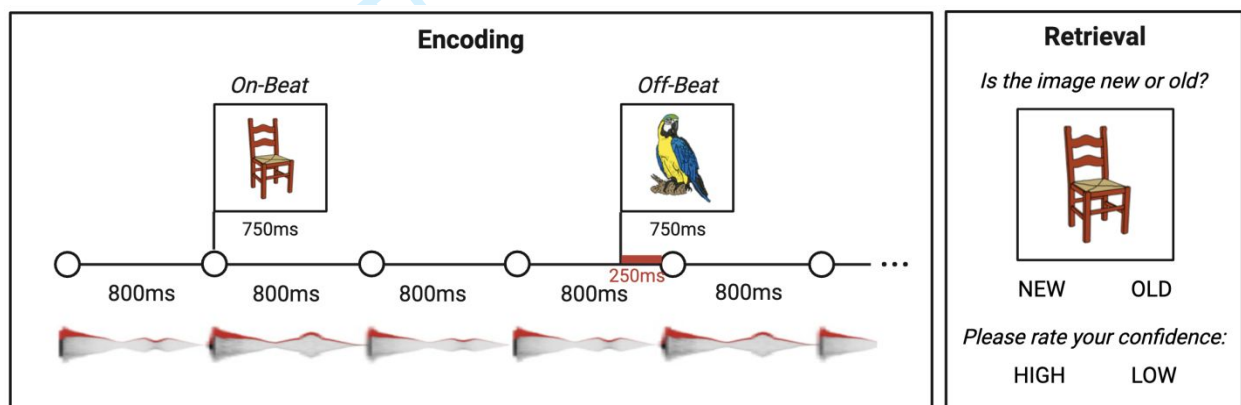


Figure 5. Experimental design for Study 2. Participants completed a single encoding (study) phase followed by a single retrieval (test) phase. During encoding, participants were shown a series of images in the context of music containing a steady 1.25 Hz beat. The beat timing is depicted using white circles above a schematic of the audio waveform of the music whose amplitude envelope is shown in red. Images were either presented synchronously (on-beat) or 250ms prior to the beat (off-beat). Each image remained on the screen for 750ms and participants were instructed to make a decision about whether the image was living or non-living. During retrieval, participants were given a self-paced memory tests where they identified if they had seen the image during the encoding task and their confidence (high, low) in their decision.

recognition memory test (in silence) in which they were shown the 120 objects from the encoding block, one at a time, intermixed with 60 novel foil objects. Participants were asked to decide whether each object had been previously seen during the encoding block (old) or not (new) and to indicate their confidence in each decision (high or low). EEG was recorded continuously throughout the encoding phase.

EEG Analysis

EEG Recording and Preprocessing

EEG was recorded from 32 channels using a BioSemi Active Two System (BioSemi, Amsterdam, Netherlands). The signal was recorded with a sampling rate of 1024 Hz and was referenced to the CMS-DRL. Two additional electrodes were placed on the mastoids and EOG was recorded from two electrodes to detect eye blinks. EEG preprocessing was completed using the EEGLab toolbox and custom MATLAB scripts. First, EEG data was referenced to the average of the mastoid electrodes. EEG signals were then downsampled to 512 Hz and filtered using a 0.1 Hz high pass and 120 Hz low pass filter. Eye artifacts were then removed from the signal using independent components analysis.

For phase-amplitude coupling analyses, EEG data was epoched into 8 second segments (approximately 97 epochs total) to allow for artifact rejection. This epoch length resulted in 10 cycles of the low-frequency oscillation (1.25 Hz) per epoch (consistent with the approach in Study 1). Epochs containing muscle artifacts were removed by visual inspection. On average, 77 epochs ($SD = 14.50$) per participant were retained after artifact rejection.

For gamma power analyses, EEG data was epoched around the presentation of the visual stimuli (-2:2s) and sorted based on the timing (on-beat v. off-beat). Epochs containing muscle artifacts were removed by visual inspection. A similar number of on-beat trials ($M = 50.42$; $SD = 7.30$) and off-beat trials ($M = 50.89$; $SD = 7.31$) retained after artifact rejection ($t(34) = -.74$, $p = .46$, $d = .12$).

Phase-Amplitude Coupling

Phase-amplitude coupling was calculated during encoding using the PACTools toolbox for MATLAB (Martínez-Cancino, 2020). Consistent with Study 1, phase-amplitude coupling was computed using the Modulation Index (MI; Tort et al., 2010). Details about the calculation

1
2
3 of the Modulation Index can be found in Study 1. In this audio-visual task, phase-amplitude
4 coupling was computed at electrode Cz. The choice to use Cz instead of electrodes PO7 and PO8
5
6 (which were used in Study 1) was motivated by the difference in modality of the entraining
7
8 stimulus (auditory rather than visual rhythm). Auditory entrainment is generally strongest in
9
10 fronto-central electrode channels (Henry et al., 2014; Nozaradan et al., 2011) and significant 1.25
11
12 Hz auditory entrainment was previously analyzed by Hickey and colleagues (2020) at electrode
13
14 Cz. For the low-frequency oscillation, the signal was filtered +/- 0.125 Hz around the rhythmic
15
16 frequency (1.25 Hz), resulting in a signal containing information between 1.125–1.375 Hz. High
17
18 frequency gamma oscillations were filtered between 30-100 Hz in 5 Hz steps (Köster et al.,
19
20 2019). As described in Study 1, MI_{surr} and MI_z values were created using a surrogate distribution
21
22 of MI values to determine statistical significance of phase-amplitude coupling and to use in
23
24 correlations with memory performance.
25
26
27
28
29

30 31 ***Gamma Power***

32
33 Gamma power at the time of stimulus presentation was computed in EEGLab between 30-
34
35 100 Hz in 1 Hz bins across the entire epoch (-2s–2s) with a resolution of 10ms using a Morlet
36
37 wavelet (7 cycles). The signal in each epoch at electrode Cz was baselined using a window of -
38
39 900ms–100ms. This baseline was selected because it allowed for one complete cycle of the 1.25
40
41 Hz oscillation. Gamma power was averaged across narrow window surrounding stimulus
42
43 presentation (-100-100ms). This window was selected in order to detect differences in on-beat
44
45 and off-beat trials given that off-beat trials are relatively close in time to the beat (250ms prior).
46
47 The -100ms to 100ms window ensured that there was no overlap between analysis windows for
48
49 on-beat and off-beat trials. Average gamma power in the low (30-60 Hz) and high (65-100 Hz)
50
51 ranges were calculated separately for on-beat and off-beat trials.
52
53
54
55
56
57
58
59
60

Statistical Analysis Plan

All statistics were completed in RStudio. Comparisons with the Modulation Index (MI_{raw} and MI_{surr}) were made using non-parametric statistics given the non-linear scale of the MI.

Analyses using normalized coupling (MI_z) and gamma power were completed using parametric statistics, except in cases where distributions were non-normally distributed. One participant was excluded from analyses involving phase-amplitude coupling, as they had coupling that was $>6SD$ above the mean.

We first tested for the presence of significant phase-amplitude coupling between low-frequency oscillations at the rhythmic frequency (1.25 Hz) and gamma amplitudes during encoding (which always occurred in the context of rhythm). A Wilcoxon Signed Rank test compared MI_{raw} values to the MI_{surr} values across the entire gamma range (30-100 Hz), and within the high gamma range (65-100 Hz) and low gamma range (30-60 Hz) separately. Next, we examined whether gamma power differed between on-beat and off-beat trials within participants by entering the gamma power at time of the visual stimulus presentation into a 2x2 repeated measures ANOVA containing factors of Gamma Band (high, low) and Timing (on-beat, off-beat). Finally, we investigated the relationship between phase-amplitude coupling, gamma power, and local effects of rhythm on memory using multiple linear regression. The difference in phase-amplitude coupling and gamma power (on-beat – off-beat) were used as predictors in the model, and the local memory effect (on-beat – off-beat) was used as the outcome variable. Bayes Factors (BF) were also computed using JASP (Version 0.17.1; JASP Team, 2023) for all null effects which were related to our hypotheses of interest.

Results

Phase-Amplitude Coupling

Significant coupling between low-frequency oscillations at the beat frequency (1.25 Hz) and gamma oscillations was present during stimulus encoding (Figure 6A; $Z = -2.40$, $p = .008$, $r = .29$). As in Study 1, this cross-frequency PAC appeared to be strongest for high gamma. Indeed, separate analysis of low gamma (30-60 Hz) and high gamma (65-100 Hz) responses confirmed that there was significant PAC between entrained oscillations and oscillations in the high gamma range ($Z = -1.95$, $p = .025$, $r = .23$) but not the low gamma range (Figure 6B-C; $Z = -0.84$, $p = .20$, $r = .10$, $BF_{10} = 1.007$).

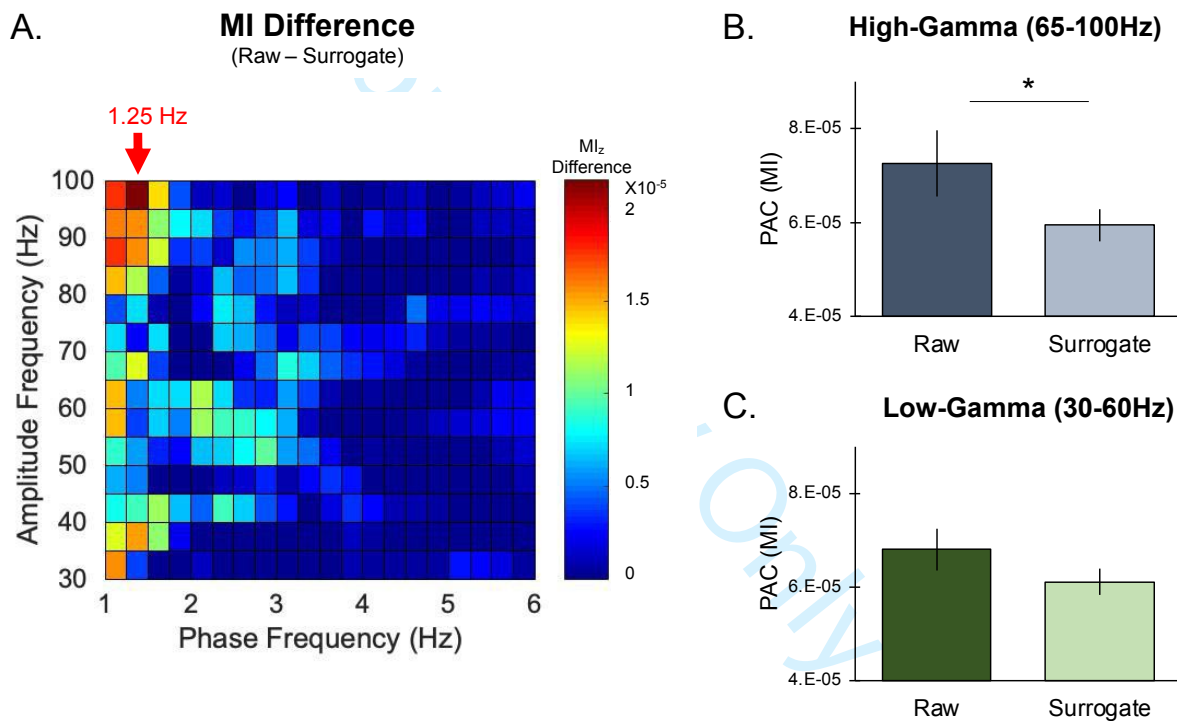


Figure 6. (A) Comodulogram displays the difference in phase-amplitude coupling (PAC; raw values – surrogate values) across the semantic decision task. Significant coupling (shown in warmer colors) is present between a range of lower (1.0-1.5 Hz) and higher (30-100 Hz) frequencies. However, peak coupling appears to occur between the entrained (1.25 Hz) oscillation and higher (80-100 Hz) frequencies. (B) Significant coupling occurred between the 1.25 Hz entrained oscillation and high-gamma (65-100 Hz) activity but, (C) not in the low-gamma range (30-60 Hz). Error bars represent SEM. * $p < .01$

Gamma Power

As predicted, gamma power at the time of stimulus presentation was greater for on-beat compared to off-beat trials (Figure 7A; $F(1,35) = 4.56, p = .040, \eta^2_p = .12$), with no main effect of Gamma Band (high, low; $F(1,35) = .31, p = .58, \eta^2_p = .01, BF10 = .158$) nor interaction between Timing (on-beat, off-beat) and Gamma Band ($F(1,35) = 1.81, p = .19, \eta^2_p = .05, BF10 = .231$). However, we were specifically interested in modulations of gamma power resulting from entrained low-frequency oscillations at the beat frequency (1.25 Hz). Since only high gamma demonstrated significant PAC, we reasoned that entrained oscillations may have a specific effect on the power of oscillations in the high gamma range. In support of this idea, PAC strength was positively associated with oscillatory power high in the gamma range ($r(33) = .39, p = .021$) (65-100 Hz; Figure 7B) and did not correlate with the power of oscillations in the low-gamma range ($r(33) = .21, p = .23, BF10 = .224$). Furthermore, post-hoc exploratory analysis revealed that this positive association between PAC and gamma power was only present for on-beat trials ($r(33) = .36, p = .036$), and was not significant for off-beat trials ($r(33) = -.23, p = .19, BF10 = .487$).

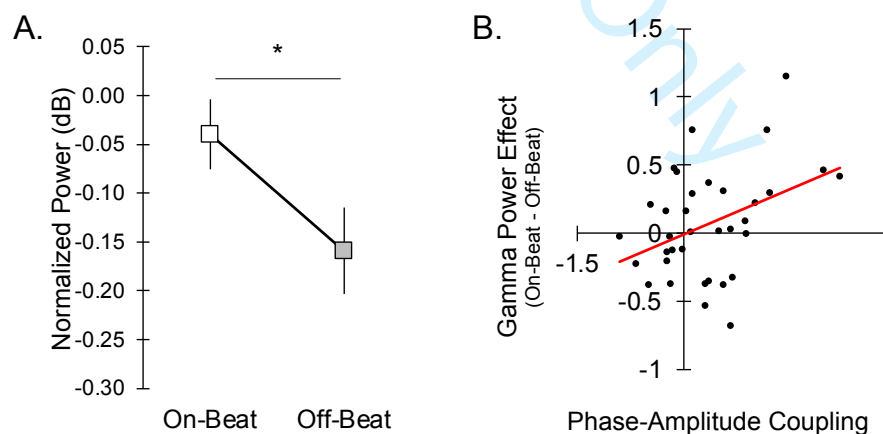


Figure 7. (A) Differences in gamma power (on-beat – off-beat). (B) At the time of stimulus presentation (-100:100ms), gamma power (30-100 Hz) is greater for on-beat compared with off-beat trials. (C) Importantly, in the high-gamma range, the strength of the coupling is related to the strength of the gamma power effects (on-beat > off-beat) in the high-gamma range. Error bars represent SEM. * $p < .05$

Brain and Behavior Relationships

Next, we investigated whether there was a relationship between PAC or gamma power and the mnemonic effects of rhythm (d' on – d' off) using multiple linear regression. The analysis was restricted to gamma oscillations in the high gamma range given that PAC and power effects were greatest for high gamma (see above). Phase-amplitude coupling was not a significant predictor of the rhythmic modulation of memory effect ($B = -.10, \beta = -.29, p = .11, BF_{10} = .379$). However, the difference in high gamma power between on-beat and off-beat trials did significantly predict the magnitude of the memory effect ($B = .23, \beta = .40, p = .032$). Specifically, a larger difference in gamma power for on-beat versus off-beat trials was associated with a greater memory benefit for on-beat versus off-beat trials. This suggests that the mnemonic effects of rhythm may not simply reflect the strength of PAC itself but the effect of PAC on the amplitude of high-frequency gamma oscillations. Post-hoc analysis confirmed there were no influential cases present (Cook's Distance < 1), the assumption of homoscedasticity was met, and multicollinearity between predictors was not present (Tolerance $> .10$; VIF < 10).

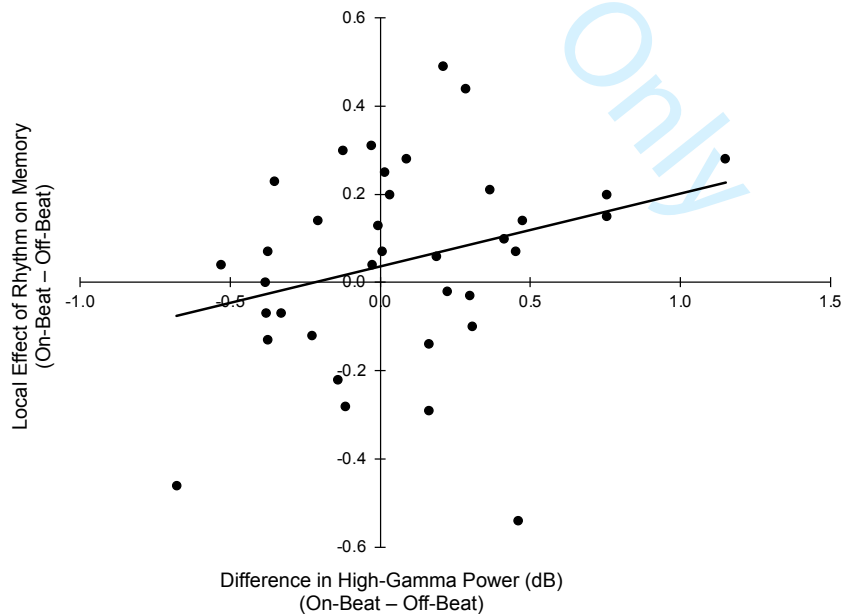


Figure 8. The difference in high-gamma phase power (dB) between on-beat and off-beat blocks showed is positively related with the local effect of rhythm on memory (d' on-beat - d' off-beat).

1
2
3
4
5
6
7
8
9
10
11
12
13
14
15
16
17
18
19
20
21
22
23
24
25
26
27
28
29
30
31
32
33
34
35
36
37
38
39
40
41
42
43
44
45
46
47
48

There has been growing recognition that environmental rhythms influence higher-order cognitive functions, such as encoding of information into long-term memory. The current study investigated potential neural mechanisms underlying this effect. Specifically, we investigated whether the effects of rhythm on memory encoding reflects the coordinated modulation of gamma oscillations by low-frequency oscillations entrained to the beat. In Study 1, we first examined this question in the context of global effects of rhythm on memory, when memory performance is enhanced for stimuli presented rhythmically compared to arrhythmically at encoding. We found that rhythmic presentation of stimuli is associated with greater phase-amplitude coupling between low-frequency oscillations at the beat frequency (1.67 Hz) and higher-frequency gamma oscillations (65-100 Hz) typically associated with episodic memory formation (Burke et al., 2014; Colgin et al., 2009; Griffiths et al., 2019). In Study 2, we next investigated this question in the context of local effects of rhythm on memory, when memory performance is enhanced for stimuli presented on-beat versus off-beat within a rhythmic context. We again found evidence for significant coupling between low-frequency oscillations at the beat frequency (1.25 Hz) and higher-frequency gamma oscillations (65-100 Hz). We also found that modulated high-frequency gamma activity was greater at the stimulus level for on-beat than off-beat trials and was positively associated with the memory benefit for on-beat versus off-beat trials. Together, these results provide novel evidence that environmental rhythms orchestrate neural activity at multiple levels during memory encoding, and that the mnemonic effects of rhythm reflect cross-frequency coupling in the brain.

49
50
51
52
53
54
55
56
57
58
59
60

The finding that entrained low-frequency oscillations influence information processing by way of modulating higher-frequency gamma oscillations complements and extends current theories of entrainment. Specifically, prior work has demonstrated that low-frequency oscillatory

1
2
3 entrainment and fluctuations in coupled gamma activity enhance the processing of relevant
4 events in the environment by creating distinct temporal windows optimized for sensory-
5 perceptual processing (rhythmic perceptual sampling) (Arnal & Giraud, 2012; Calderone et al.,
6 2014; Lakatos et al., 2008; Schroeder & Lakatos, 2009). Here, we find that entrained oscillations
7 and coupled gamma activity also create temporal windows optimized for memory encoding
8 (mnemonic sampling). These results support the proposal that rhythm biases the brain into a
9 more efficient “rhythmic mode” of processing that can influence both perception and cognition
10 (Hickey & Race, 2021; Schroeder & Lakatos, 2009). Furthermore, while prior work has
11 highlighted the importance of entrained oscillations for memory encoding (Hickey, Merseal, et
12 al., 2020; A. Jones & Ward, 2019), here we specify a more precise mechanism by which this
13 may occur. That is, our results suggest that it is not the entrained oscillations themselves that
14 modulate memory encoding, but the coordination of higher-frequency activity by entrained
15 oscillations. This adds to a growing body of literature emphasizing the importance of cross-
16 frequency phase-amplitude coupling, and particularly the coupling of gamma oscillations, for the
17 encoding of information into long-term memory (e.g., Köster et al., 2019).

18
19 An important aspect of the current results is that they provide evidence of similar
20 memory entrainment mechanisms for both visual rhythms (Study 1) as well as auditory rhythms
21 (Study 2), despite differences in task design and entraining frequency (1.67 Hz and 1.25 Hz,
22 respectively). This suggests that entrainment may not need to occur in a specific modality or at a
23 specific frequency, but instead could be a more general way for the brain leverage statistical
24 regularities in the environment to optimize neural responsivity across time. Future work could
25 further test this hypothesis and the generalizability of these results by investigating the effects of
26
27
28
29
30
31
32
33
34
35
36
37
38
39
40
41
42
43
44
45
46
47
48
49
50
51
52
53
54
55
56
57
58
59
60

1
2
3 different entraining modalities (e.g., effects of visual rhythms on auditory encoding) and
4
5 entraining frequencies (e.g., theta rhythms) on memory performance.
6
7

8 Interestingly, in both Study 1 and Study 2, phase-amplitude coupling effects in the
9
10 context of rhythm were most prominent for oscillations in the high-gamma range (65-100 Hz). A
11
12 large body of work has demonstrated that gamma activity in different frequency ranges may
13
14 result from different underlying mechanisms (Colgin et al., 2009; Crone et al., 2011), and has
15
16 suggested that higher-frequency gamma activity may be closely related to attention and memory
17
18 encoding (Castelhano et al., 2014; Chacko et al., 2018; Colgin et al., 2009; Griffiths et al., 2019;
19
20 Ray et al., 2008). For example, a recent study by Chacko et al. (2018) found that coupling
21
22 between low-frequency oscillations and gamma oscillations in the higher gamma range were
23
24 associated with attentional orienting, whereas coupling between low-frequency oscillations and
25
26 oscillations in the lower gamma range was associated with response speeds during a cued spatial
27
28 attention task. A similar pattern has been observed in studies of gamma power, where high
29
30 gamma activity has also been elicited by attentional cues in a conditional visuomotor task
31
32 (Brovelli et al., 2005). It has been proposed that coupling between low-frequency oscillations
33
34 and high-gamma power may be related to changes in synaptic strength (LTP/LTD) and
35
36 attentional orienting that is relevant for learning and memory (Canolty & Knight, 2010;
37
38 Schroeder & Lakatos, 2009). Indeed, the coupling of theta and high-gamma oscillations and the
39
40 synchrony of gamma activity within the prefrontal cortex and hippocampus has been associated
41
42 with spatial working memory performance (Alekseichuk et al., 2016; Carver et al., 2019;
43
44 Yamamoto et al., 2014). Additionally, cross frequency coupling between low-frequency (theta)
45
46 and high-frequency (high-gamma) oscillations within the hippocampus has been linked with
47
48 encoding processes, whereas coupling between theta and low-gamma is more tightly associated
49
50
51
52
53
54
55
56
57
58
59
60

1
2
3 with memory retrieval (Colgin et al., 2009; Griffiths et al., 2019). Together with the current
4
5 results, this suggests that coupled oscillations in the high gamma range may be particularly
6
7 relevant for memory encoding and for directing attention to particular moments in time in order
8
9 to enhance encoding.
10

11
12 Another important aspect of the current results is that they link entrained cross-frequency
13
14 PAC to the mnemonic effects of rhythm at both the global level (Study 1) and the local level
15
16 (Study 2). However, we did not find a consistent brain-behavior relationship between PAC and
17
18 the mnemonic benefits of rhythm across studies. In Study 1, the lack of a relationship between
19
20 the magnitude of phase-amplitude coupling and the global effects of rhythm on memory
21
22 performance might reflect a lack of sensitivity at the behavioral or neural level. Study 1 utilized a
23
24 blocked design, where the mnemonic benefit of rhythm was defined as the difference in memory
25
26 between rhythmic and arrhythmic blocks. Previous studies have found that the effects of rhythm
27
28 on memory change over time and may be most pronounced in the first blocks (Johndro et al.,
29
30 2019). Therefore, averaging across blocks could have reduced our ability to detect subtle effects
31
32 of rhythm on memory performance. Similarly, PAC was only evaluated at the block level, rather
33
34 than at the trial level. Therefore, faster fluctuations in coupled gamma activity may have been
35
36 difficult to detect or may be more closely associated with local effects of rhythm on memory.
37
38 Indeed, in the original study by Jones and Ward (2019), entrainment strength was also not
39
40 associated with the global effects of rhythm on memory performance.
41
42
43
44
45

46
47 In contrast, a significant positive relationship was observed in Study 2 between the
48
49 magnitude of entrained gamma power and the mnemonic effects of rhythm at the local level
50
51 (memory benefit for on-beat vs. off-beat trials). This parallels the results observed in the original
52
53 study by Hickey, Merseal, and colleagues (2020), in which entrainment strength was also
54
55
56
57
58
59
60

1
2
3 positively correlated with memory performance, and suggests that brain-behavior relationships
4 may be more easily detected using more fine-grained measurements and manipulations of
5
6 rhythmic effects on behavior and neural processing. Interestingly, the magnitude of entrained
7
8 PAC did not positively correlate with the mnemonic benefits of rhythm, but the magnitude of
9
10 gamma power did. This suggests that it may not be the coupling itself that is relevant for
11
12 encoding but rather the timing of gamma activity relative to the rhythmic stream. This was
13
14 surprising given the large body of work which has found that coupled gamma oscillations
15
16 influence memory encoding more broadly (Canolty et al., 2006; Frieze et al., 2013; Köster et al.,
17
18 2019; Lega et al., 2016; Tort et al., 2008). However, these studies have typically focused on
19
20 theta-gamma coupling (rather than *delta*-gamma coupling) and have not investigated the effect of
21
22 coupling on encoding *at specific moments in time*. Future work should investigate whether
23
24 significant correlations are present between entrained PAC and memory performance at the
25
26 global or local level when rhythms occur in the theta range. This would help to further extend
27
28 theoretical models from the memory domain that emphasize theta-gamma coupling (e.g., theta-
29
30 gamma neural code; Lisman & Jensen, 2013).

31 32 33 34 35 36 37 **Limitations and Future Directions**

38
39
40 The current study was a reanalysis of two existing datasets collected by Jones and Ward
41
42 (2019) and Hickey, Merseal, et al. (2020) . These studies were selected because they allowed us
43
44 to investigate the effect of coupled oscillations on memory performance at both the global and
45
46 local levels. However, methodological differences across studies make it difficult to directly
47
48 compare the results. For example, one major difference between the two paradigms (as
49
50 mentioned previously) was the visual versus auditory entraining stimuli. Although including
51
52 different entraining modalities was a unique feature of this study, it also created differences in
53
54
55
56
57
58
59
60

1
2
3 whether entrainment was having unimodal or cross-modal effects on memory encoding (since
4 memory was for visual images in both paradigms). In addition, Jones and Ward (2019) used a
5 repeated study-test design whereas participants in Hickey, Merseal, et al. (2020) only had one
6 study block and one surprise subsequent memory test. Future work could more directly compare
7 the effects of rhythm on global versus local processing by using more similar paradigms.
8
9
10
11
12
13

14
15 Future work should also explore whether oscillations in other frequency bands may also
16 be relevant for rhythmic effects on memory. For example, theta-gamma coupling, which has
17 been frequently associated with memory encoding (Buzsáki & Wang, 2012; Canolty & Knight,
18 2010; Lisman & Jensen, 2013), may be nested within entrained delta oscillations (Lakatos et al.,
19 2005, 2008). The dynamic orchestration of oscillations outside the delta, theta, and gamma bands
20 could also contribute to the temporal structuring of episodic memory. For example, alpha
21 oscillations are thought to play an important role in the gating selective attention and are known
22 to play role in memory formation (Hanslmayr & Staudigl, 2014; Voytek et al., 2010). Beta
23 oscillations have also been implicated in memory tasks and are thought to control shifts in
24 attention and neural excitability according to temporal expectations (Buschman et al., 2012;
25 Cravo et al., 2011; Fiebelkorn & Kastner, 2019; Hanslmayr & Staudigl, 2014). In the language
26 domain, interactions between the phase and amplitude of nested theta, gamma, delta and beta
27 oscillations have been proposed to provide a dynamic neural code, or “neurocomputational
28 multiplexing”, central for structuring language (Murphy, 2020). Future research should
29 investigate the degree to which nested oscillations across multiple frequency bands might also
30 adaptively structure memory formation.
31
32
33
34
35
36
37
38
39
40
41
42
43
44
45
46
47
48
49
50

51 **Data Availability**

52
53 The data that support the findings of this study are available online through Open Science
54 Framework (Study 1: <https://osf.io/hv4j8/>; Study 2: <https://osf.io/wzc2g>).
55
56
57
58
59
60

Author Contributions

Paige Hickey Townsend: Conceptualization; Methodology; Formal analysis; Investigation; Writing - original draft; Writing – review & editing; Visualization. Alexander Jones: Methodology; Formal analysis; Investigation; Writing – review & editing. Aniruddh D. Patel: Methodology; Writing - review & editing; Supervision; Funding acquisition. Elizabeth Race: Conceptualization; Methodology; Formal analysis; Investigation; Resources; Writing - original draft; Writing – review & editing; Visualization, Supervision; Project administration; Funding acquisition.

Acknowledgements

The authors would like to acknowledge Emma Ward and Alex Isac for their role in data collection and behavioral data analysis from Study 1, David DiStefano, Hannah Merseal, Catherine Gross, Alexandra Cohen, and Annie Barnett-Young for their assistance with data collection on Study 2, and Ayanna Thomas for her feedback on earlier versions of this work.

Funding

This research was funded (in part) by a grant from the GRAMMY Museum®.

References

- Alekseichuk, I., Turi, Z., Amador de Lara, G., Antal, A., & Paulus, W. (2016). Spatial working memory in humans depends on theta and high gamma synchronization in the prefrontal cortex. *Current Biology*, *26*(12), 1513–1521. <https://doi.org/10.1016/j.cub.2016.04.035>
- Arnal, L. H., & Giraud, A. L. (2012). Cortical oscillations and sensory predictions. *Trends in Cognitive Sciences*, *16*(7), 390–398. <https://doi.org/10.1016/j.tics.2012.05.003>
- Barnhart, A. S., Ehlert, M. J., Goldinger, S. D., & Mackey, A. D. (2018). Cross-modal attentional entrainment: Insights from magicians. *Attention, Perception, & Psychophysics*, *80*(5), 1240–1249. <https://doi.org/10.3758/s13414-018-1497-8>
- Bartoli, E., Bosking, W., Chen, Y., Li, Y., Sheth, S. A., Beauchamp, M. S., Yoshor, D., & Foster, B. L. (2019). Functionally distinct gamma range activity revealed by stimulus tuning in human visual cortex. *Current Biology*, *29*(20), 3345–3358.e7. <https://doi.org/10.1016/j.cub.2019.08.004>
- Besle, J., Schevon, C. A., Mehta, A. D., Lakatos, P., Goodman, R. R., McKhann, G. M., Emerson, R. G., & Schroeder, C. E. (2011). Tuning of the human neocortex to the temporal dynamics of attended events. *The Journal of Neuroscience*, *31*(9), 3176–3185. <https://doi.org/10.1523/JNEUROSCI.4518-10.2011>
- Bolger, D., Trost, W., & Schön, D. (2013). Rhythm implicitly affects temporal orienting of attention across modalities. *Acta Psychologica (Amst)*, *142*(2), 238–244. <https://doi.org/10.1016/j.actpsy.2012.11.012>
- Brovelli, A., Lachaux, J. P., Kahane, P., & Boussaoud, D. (2005). High gamma frequency oscillatory activity dissociates attention from intention in the human premotor cortex. *Neuroimage*, *28*(1), 154–164. <https://doi.org/10.1016/j.neuroimage.2005.05.045>

- 1
2
3 Burke, J. F., Long, N. M., Zaghoul, K. A., Sharan, A. D., Sperling, M. R., & Kahana, M. J.
4
5 (2014). Human intracranial high-frequency activity maps episodic memory formation in
6
7 space and time. *NeuroImage*, *85 Pt 2*, 834–843.
8
9 <https://doi.org/10.1016/j.neuroimage.2013.06.067>
10
11
12 Buschman, T. J., Denovellis, E. L., Diogo, C., Bullock, D., & Miller, E. K. (2012). Synchronous
13
14 oscillatory neural ensembles for rules in the prefrontal cortex. *Neuron*, *76*(4), 838–846.
15
16 <https://doi.org/10.1016/j.neuron.2012.09.029>
17
18
19 Buzsáki, G. (2006). *Rhythms of the Brain*. Oxford University Press.
20
21 <https://doi.org/10.1093/acprof:oso/9780195301069.001.0001>
22
23
24 Buzsáki, G., & Wang, X. J. (2012). Mechanisms of gamma oscillations. *Annual Review of*
25
26 *Neuroscience*, *35*, 203–225. <https://doi.org/10.1146/annurev-neuro-062111-150444>
27
28
29 Calderone, D. J., Lakatos, P., Butler, P. D., & Castellanos, F. X. (2014). Entrainment of neural
30
31 oscillations as a modifiable substrate of attention. *Trends in Cognitive Sciences*, *18*(6),
32
33 300–309. <https://doi.org/10.1016/j.tics.2014.02.005>
34
35
36 Canolty, R. T., Edwards, E., Dalal, S. S., Soltani, M., Nagarajan, S. S., Kirsch, H. E., Berger, M.
37
38 S., Barbaro, N. M., & Knight, R. T. (2006). High gamma power is phase-locked to theta
39
40 oscillations in human neocortex. *Science*, *313*(5793), 1626–1628.
41
42 <https://doi.org/10.1126/science.1128115>
43
44
45 Canolty, R. T., & Knight, R. T. (2010). The functional role of cross-frequency coupling. *Trends*
46
47 *in Cognitive Sciences*, *14*(11), 506–515. <https://doi.org/10.1016/j.tics.2010.09.001>
48
49
50 Carver, F. W., Rubinstein, D. Y., Gerlich, A. H., Fradkin, S. I., Holroyd, T., & Coppola, R.
51
52 (2019). Prefrontal high gamma during a magnetoencephalographic working memory task.
53
54 *Human Brain Mapping*, *40*(6), 1774–1785. <https://doi.org/10.1002/hbm.24489>
55
56
57
58
59
60

- 1
2
3 Castelhano, J., Duarte, I. C., Wibral, M., Rodriguez, E., & Castelo-Branco, M. (2014). The dual
4
5 facet of gamma oscillations: Separate visual and decision making circuits as revealed by
6
7 simultaneous EEG/fMRI. *Human Brain Mapping, 35*(10), 5219–5235.
8
9
10 <https://doi.org/10.1002/hbm.22545>
11
- 12 Chacko, R. V., Kim, B., Jung, S. W., Daitch, A. L., Roland, J. L., Metcalf, N. V., Corbetta, M.,
13
14 Shulman, G. L., & Leuthardt, E. C. (2018). Distinct phase-amplitude couplings
15
16 distinguish cognitive processes in human attention. *NeuroImage, 175*, 111–121.
17
18
19 <https://doi.org/10.1016/j.neuroimage.2018.03.003>
20
- 21 Colgin, L. L., Denninger, T., Fyhn, M., Hafting, T., Bonnevie, T., Jensen, O., Moser, M. B., &
22
23 Moser, E. I. (2009). Frequency of gamma oscillations routes flow of information in the
24
25 hippocampus. *Nature, 462*(7271), 353–357. <https://doi.org/10.1038/nature08573>
26
27
- 28 Cravo, A. M., Rohenkohl, G., Wyart, V., & Nobre, A. C. (2011). Endogenous modulation of low
29
30 frequency oscillations by temporal expectations. *Journal of Neurophysiology, 106*(6),
31
32 2964–2972. <https://doi.org/10.1152/jn.00157.2011>
33
34
- 35 Crone, N. E., Korzeniewska, A., & Franaszczuk, P. J. (2011). Cortical gamma responses:
36
37 Searching high and low. *International Journal of Psychophysiology, 79*(1), 9–15.
38
39
40 <https://doi.org/10.1016/j.ijpsycho.2010.10.013>
41
- 42 Delorme, A., & Makeig, S. (2004). EEGLAB: An open source toolbox for analysis of single-trial
43
44 EEG dynamics including independent component analysis. *Journal of Neuroscience*
45
46 *Methods, 134*(1), 9–21. <https://doi.org/10.1016/j.jneumeth.2003.10.009>
47
48
- 49 Ding, N., Patel, A., Chen, L., Butler, H., Luo, C., & Poeppell, D. (2017). Temporal modulations
50
51 in speech and music. *Neuroscience & Biobehavioral Reviews, 81*, 181–187.
52
53
54 <https://doi.org/doi:10.1016/j.neubiorev.2017.02.011>
55
56
57
58
59
60

- 1
2
3 Ding, N., & Simon, J. Z. (2014). Cortical entrainment to continuous speech: Functional roles and
4 interpretations. *Frontiers in Human Neuroscience*, *8*, 311.
5
6 <https://doi.org/doi.org/10.3389/fnhum.2014.00311>
7
8
9
10 Escoffier, N., Sheng, D. Y., & Schirmer, A. (2010). Unattended musical beats enhance visual
11 processing. *Acta Psychologica (Amst)*, *135*(1), 12–16.
12
13 <https://doi.org/10.1016/j.actpsy.2010.04.005>
14
15
16
17 Fiebelkorn, I. C., & Kastner, S. (2019). A rhythmic theory of attention. *Trends in Cognitive*
18 *Sciences*, *23*(2), 87–101. <https://doi.org/10.1016/j.tics.2018.11.009>
19
20
21 Friese, U., Köster, M., Hassler, U., Martens, U., Trujillo-Barreto, N., & Gruber, T. (2013).
22 Successful memory encoding is associated with increased cross-frequency coupling
23 between frontal theta and posterior gamma oscillations in human scalp-recorded EEG.
24 *NeuroImage*, *66*, 642–647. <https://doi.org/10.1016/j.neuroimage.2012.11.002>
25
26
27
28
29
30
31 Griffiths, B. J., Parish, G., Roux, F., Michelmann, S., van der Plas, M., Kolibius, L. D.,
32 Chelvarajah, R., Rollings, D. T., Sawlani, V., Hamer, H., Gollwitzer, S., Kreiselmeyer,
33 G., Staresina, B., Wimber, M., & Hanslmayr, S. (2019). Directional coupling of slow and
34 fast hippocampal gamma with neocortical alpha/beta oscillations in human episodic
35 memory. *Proceedings of the National Academy of Sciences of the United States of*
36 *America*, *116*(43), 21834–21842. <https://doi.org/10.1073/pnas.1914180116>
37
38
39
40
41
42
43
44
45 Hanslmayr, S., & Staudigl, T. (2014). How brain oscillations form memories—A processing
46 based perspective on oscillatory subsequent memory effects. *NeuroImage*, *85 Pt 2*, 648–
47 655. <https://doi.org/10.1016/j.neuroimage.2013.05.121>
48
49
50
51 Henry, M. J., Herrmann, B., & Obleser, J. (2014). Entrained neural oscillations in multiple
52 frequencybands comodulate behavior. *Proceedings of the National Academy of Sciences*
53
54
55
56
57
58
59
60

1
2
3 of the United States of America, 111(41), 14935–14940.

4
5 <https://doi.org/10.1073/pnas.1408741111>

6
7
8 Hickey, P., Barnett-Young, A., Patel, A. D., & Race, E. (2020). Environmental rhythms
9 orchestrate neural activity at multiple stages of processing during memory encoding:
10 Evidence from event-related potentials. *PLoS One*, 15(11), e0234668.

11
12
13 <https://doi.org/10.1371/journal.pone.0234668>

14
15
16
17 Hickey, P., Merseal, H., Patel, A. D., & Race, E. (2020). Memory in time: Neural tracking of
18 low-frequency rhythm dynamically modulates memory formation. *NeuroImage*, 213,
19 116693. <https://doi.org/10.1016/j.neuroimage.2020.116693>

20
21
22
23
24 Hickey, P., & Race, E. (2021). Riding the slow wave: Exploring the role of entrained low-
25 frequency oscillations in memory formation. *Neuropsychologia*, 160, 107962.

26
27
28 <https://doi.org/10.1016/j.neuropsychologia.2021.107962>

29
30
31 Hülsemann, M. J., Naumann, E., & Rasch, B. (2019). Quantification of phase-amplitude
32 coupling in neuronal oscillations: Comparison of phase-locking value, mean vector
33 length, modulation index, and generalized-linear-modeling-cross-frequency-coupling.
34 *Frontiers in Neuroscience*, 13, 573. <https://doi.org/10.3389/fnins.2019.00573>

35
36
37
38
39
40 Jensen, O., Kaiser, J., & Lachaux, J. P. (2007). Human gamma-frequency oscillations associated
41 with attention and memory. *Trends in Neurosciences*, 30(7), 317–324.

42
43
44 <https://doi.org/10.1016/j.tins.2007.05.001>

45
46
47 Johndro, H., Jacobs, L., Patel, A. D., & Race, E. (2019). Temporal predictions provided by
48 musical rhythm influence visual memory encoding. *Acta Psychologica (Amst)*, 200,
49 102923. <https://doi.org/10.1016/j.actpsy.2019.102923>

- 1
2
3 Jones, A., & Ward, E. V. (2019). Rhythmic temporal structure at encoding enhances recognition
4 memory. *Journal of Cognitive Neuroscience*, *31*(10), 1549–1562.
5
6 https://doi.org/10.1162/jocn_a_01431
7
8
9
10 Jones, A., Ward, E. V., Csiszer, E. L., & Szymczak, J. (2022). Temporal Expectation Improves
11 Recognition Memory for Spatially Attended Objects. *Journal of Cognitive Neuroscience*,
12 *34*(9), 1616–1629. https://doi.org/10.1162/jocn_a_01872
13
14
15
16
17 Jones, M. R. (2019). *Time Will Tell: A Theory of Dynamic Attending*. Oxford University Press.
18
19 <https://doi.org/10.1093/oso/9780190618216.003.0001>
20
21
22 Jones, M. R., & Boltz, M. (1989). Dynamic attending and responses to time. *Psychological*
23 *Review*, *96*(3), 459–491. <https://doi.org/10.1037/0033-295x.96.3.459>
24
25
26 Jones, M. R., Moynihan, H., MacKenzie, N., & Puente, J. (2002). Temporal aspects of stimulus-
27 driven attending in dynamic arrays. *Psychological Science*, *13*(4), 313–319.
28
29 <https://doi.org/10.1111/1467-9280.00458>
30
31
32
33 Keitel, A., Ince, R. A. A., Gross, J., & Kayser, C. (2017). Auditory cortical delta-entrainment
34 interacts with oscillatory power in multiple fronto-parietal networks. *NeuroImage*, *147*,
35 32–42. <https://doi.org/10.1016/j.neuroimage.2016.11.062>
36
37
38
39
40 Köster, M., Martens, U., & Gruber, T. (2019). Memory entrainment by visually evoked theta-
41 gamma coupling. *NeuroImage*, *188*, 181–187.
42
43 <https://doi.org/10.1016/j.neuroimage.2018.12.002>
44
45
46
47 Kulkarni, M., & Hannula, D. E. (2021). Temporal Regularity May Not Improve Memory for
48 Item-Specific Detail. *Frontiers in Psychology*, *12*.
49
50 <https://www.frontiersin.org/articles/10.3389/fpsyg.2021.623402>
51
52
53
54
55
56
57
58
59
60

- 1
2
3 Lakatos, P., Karmos, G., Mehta, A. D., Ulbert, I., & Schroeder, C. E. (2008). Entrainment of
4 neuronal oscillations as a mechanism of attentional selection. *Science*, *320*(5872), 110–
5 113. <https://doi.org/10.1126/science.1154735>
6
7
8
9
10 Lakatos, P., Shah, A. S., Knuth, K. H., Ulbert, I., Karmos, G., & Schroeder, C. E. (2005). An
11 oscillatory hierarchy controlling neuronal excitability and stimulus processing in the
12 auditory cortex. *Journal of Neurophysiology*, *94*(3), 1904–1911.
13
14
15
16
17 <https://doi.org/10.1152/jn.00263.2005>
18
19 Large, E. W., & Jones, M. R. (1999). The dynamics of attending: How people track time-varying
20 events. *Psychological Review*, *106*(1), 40. <https://doi.org/10.1037/0033-295X.106.1.119>
21
22
23
24 Lega, B., Burke, J., Jacobs, J., & Kahana, M. J. (2016). Slow-theta-to-gamma phase-amplitude
25 coupling in human hippocampus supports the formation of new episodic memories.
26
27
28
29 *Cerebral Cortex*, *26*(1), 268–278. <https://doi.org/10.1093/cercor/bhu232>
30
31 Lisman, J. E., & Jensen, O. (2013). The theta-gamma neural code. *Neuron*, *77*(6), 1002–1016.
32
33
34 <https://doi.org/10.1016/j.neuron.2013.03.007>
35
36 Mariscal, M. G., Levin, A. R., Gabard-Durnam, L. J., Xie, W., Tager-Flusberg, H., & Nelson, C.
37
38 A. (2021). EEG phase-amplitude coupling strength and phase preference: Association
39 with age over the first three years after birth. *ENeuro*, *8*(3).
40
41
42
43 <https://doi.org/10.1523/ENEURO.0264-20.2021>
44
45 Martínez-Cancino, R., Delorme, A. ., Kreutz-Delgado, K. ., Makeig, S. (2020). *Computing phase*
46
47 *amplitude coupling in EEGLAB: PACTools*. 387–394.
48
49
50 <https://doi.org/10.1109/BIBE50027.2020.00070>
51
52 Murphy, E. (2020). *The Oscillatory Nature of Language*. Cambridge University Press.
53
54
55
56
57
58
59
60

- 1
2
3 Nozaradan, S., Peretz, I., & Keller, P. E. (2016). Individual differences in rhythmic cortical
4
5 entrainment correlate with predictive behavior in sensorimotor synchronization. *Scientific*
6
7 *Reports*, 6, 20612. <https://doi.org/10.1038/srep20612>
8
9
- 10 Nozaradan, S., Peretz, I., Missal, M., & Mouraux, A. (2011). Tagging the Neuronal Entrainment
11
12 to Beat and Meter. *Journal of Neuroscience*, 31(28), 10234–10240.
13
14 <https://doi.org/10.1523/JNEUROSCI.0411-11.2011>
15
16
- 17 O’Connell, M. N., Barczak, A., Ross, D., McGinnis, T., Schroeder, C. E., & Lakatos, P. (2015).
18
19 Multi-scale entrainment of coupled neuronal oscillations in primary auditory cortex.
20
21 *Frontiers in Human Neuroscience*, 9, 655. <https://doi.org/10.3389/fnhum.2015.00655>
22
23
- 24 Osipova, D., Takashima, A., Oostenveld, R., Fernández, G., Maris, E., & Jensen, O. (2006).
25
26 Theta and gamma oscillations predict encoding and retrieval of declarative memory. *The*
27
28 *Journal of Neuroscience*, 26(28), 7523–7531. [https://doi.org/10.1523/JNEUROSCI.1948-](https://doi.org/10.1523/JNEUROSCI.1948-06.2006)
29
30 06.2006
31
32
- 33 Ray, S., Niebur, E., Hsiao, S. S., Sinai, A., & Crone, N. E. (2008). High-frequency gamma
34
35 activity (80-150Hz) is increased in human cortex during selective attention. *Clinical*
36
37 *Neurophysiology*, 119(1), 116–133. <https://doi.org/10.1016/j.clinph.2007.09.136>
38
39
- 40 Rieder, M. K., Rahm, B., Williams, J. D., & Kaiser, J. (2011). Human gamma-band activity and
41
42 behavior. *International Journal of Psychophysiology*, 79(1), 39–48.
43
44 <https://doi.org/10.1016/j.ijpsycho.2010.08.010>
45
46
- 47 Sadeh, B., Szczepanski, S. M. ., Knight, R. T. (2014). Oscillations and behavior: The role of
48
49 phase-amplitude coupling in cognition. In G. R. Mangun (Ed.), *Cognitive*
50
51 *Electrophysiology of Attention: Signals of the Mind* (pp. 268–282). Elsevier.
52
53
54
55
56
57
58
59
60

- 1
2
3 Schroeder, C. E., & Lakatos, P. (2009). Low-frequency neuronal oscillations as instruments of
4 sensory selection. *Trends in Neurosciences*, *32*(1), 9–18.
5
6 <https://doi.org/10.1016/j.tins.2008.09.012>
7
8
9
10 Sederberg, P. B., Kahana, M. J., Howard, M. W., Donner, E. J., & Madsen, J. R. (2003). Theta
11 and gamma oscillations during encoding predict subsequent recall. *The Journal of*
12 *Neuroscience*, *23*(34), 10809–10814. [https://doi.org/10.1523/JNEUROSCI.23-34-](https://doi.org/10.1523/JNEUROSCI.23-34-10809.2003)
13 [10809.2003](https://doi.org/10.1523/JNEUROSCI.23-34-10809.2003)
14
15
16
17
18
19 Sederberg, P. B., Schulze-Bonhage, A., Madsen, J. R., Bromfield, E. B., McCarthy, D. C.,
20 Brandt, A., Tully, M. S., & Kahana, M. J. (2007). Hippocampal and neocortical gamma
21 oscillations predict memory formation in humans. *Cerebral Cortex*, *17*(5), 1190–1196.
22
23
24 <https://doi.org/10.1093/cercor/bhl030>
25
26
27
28
29 Shen, L., Lu, X., Yuan, X., Hu, R., Wang, Y., & Jiang, Y. (2023). Cortical encoding of rhythmic
30 kinematic structures in biological motion. *NeuroImage*, *268*.
31
32 <https://doi.org/10.1016/j.neuroimage.2023.119893>
33
34
35
36 Thavabalasingam, S., O’Neil, E. B., Zeng, Z., & Lee, A. C. (2015). Recognition memory is
37 improved by a structured temporal framework during encoding. *Frontiers in Psychology*,
38 *6*, 2062. <https://doi.org/10.3389/fpsyg.2015.02062>
39
40
41
42
43 Tort, A. B., Komorowski, R., Eichenbaum, H., & Kopell, N. (2010). Measuring phase-amplitude
44 coupling between neuronal oscillations of different frequencies. *Journal of*
45 *Neurophysiology*, *104*(2), 1195–1210. <https://doi.org/10.1152/jn.00106.2010>
46
47
48
49
50 Tort, A. B., Kramer, M. A., Thorn, C., Gibson, D. J., Kubota, Y., Graybiel, A. M., & Kopell, N.
51 J. (2008). Dynamic cross-frequency couplings of local field potential oscillations in rat
52 striatum and hippocampus during performance of a T-maze task. *Proceedings of the*
53
54
55
56
57
58
59
60

1
2
3 *National Academy of Sciences of the United States of America*, 105(51), 20517–20522.

4
5 <https://doi.org/10.1073/pnas.0810524105>

6
7
8 Trimper, J. B., Galloway, C. R., Jones, A. C., Mandi, K., & Manns, J. R. (2017). Gamma
9
10 oscillations in rat hippocampal subregions dentate gyrus, CA3, CA1, and subiculum
11
12 underlie associative memory encoding. *Cell Reports*, 21(9), 2419–2432.

13
14
15 <https://doi.org/10.1016/j.celrep.2017.10.123>

16
17 Voytek, B., Canolty, R. T., Shestyuk, A., Crone, N. E., Parvizi, J., & Knight, R. T. (2010). Shifts
18
19 in gamma phase-amplitude coupling frequency from theta to alpha over posterior cortex
20
21 during visual tasks. *Frontiers in Human Neuroscience*, 4, 191.

22
23
24 <https://doi.org/10.3389/fnhum.2010.00191>

25
26 Yamamoto, J., Suh, J., Takeuchi, D., & Tonegawa, S. (2014). Successful execution of working
27
28 memory linked to synchronized high-frequency gamma oscillations. *Cell*, 157(4), 845–
29
30 857. <https://doi.org/10.1016/j.cell.2014.04.009>

31
32
33
34
35
36
37
38
39
40
41
42
43
44
45
46
47
48
49
50
51
52
53
54
55
56
57
58
59
60

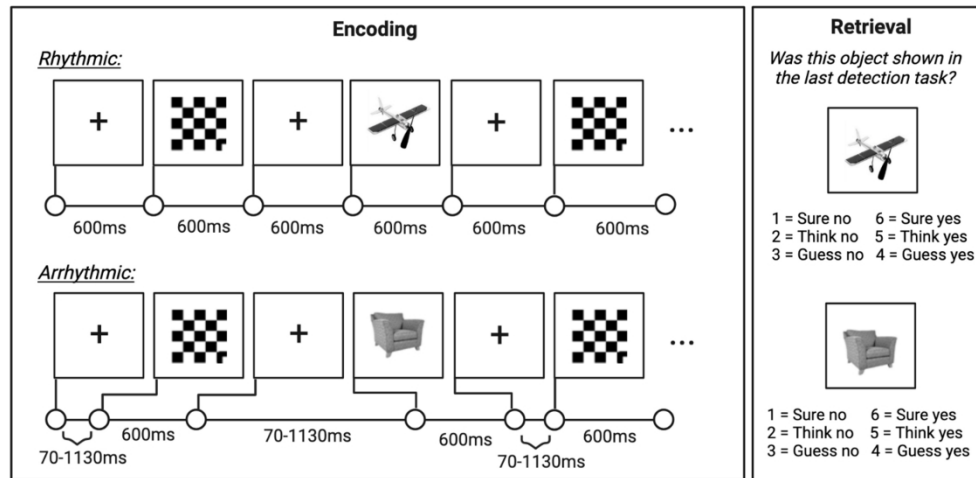


Figure 1. Experimental design for Study 1. Participants completed 6 blocks of encoding and retrieval (3 rhythmic; 3 arrhythmic). During encoding, participants were shown a series of images and checkerboards separated by fixation crosses and instructed to press the space bar each time an animal appeared. Images remained on the screen for 600ms. In rhythmic blocks, the interstimulus interval (ISI) was always 600ms, while in arrhythmic blocks the ISI was jittered between 70-1130ms. Example timelines of stimulus presentation during encoding are illustrated in the first panel. During retrieval, participants were given self-paced memory tests where they were presented with old and new images and indicated if they had seen the image during the preceding detection (encoding) task and their confidence in their memory decision.

431x210mm (144 x 144 DPI)

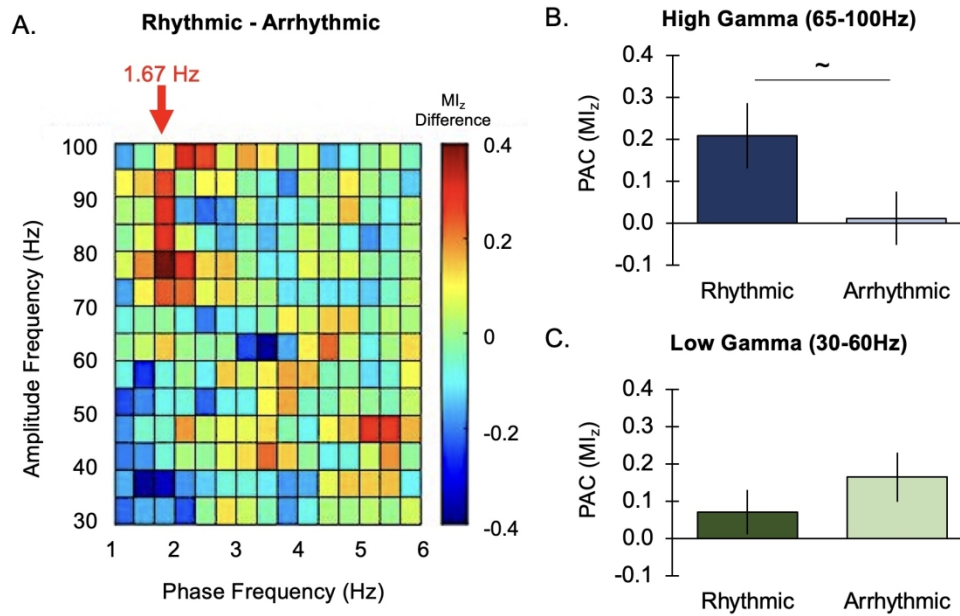


Figure 2. The difference in normalized Phase-Amplitude Coupling (PAC; measured by MI_z) between rhythmic and arrhythmic contexts. (A) The comodulogram depicts the difference in PAC between contexts (rhythmic – arrhythmic), where the third column displays coupling at the entraining frequency (1.67 Hz). (B) There was numerically greater phase-amplitude coupling at the entrained (1.67 Hz) frequency in the high-gamma (65–100 Hz) range, (C) but not in the low-gamma (30–60 Hz) range. Error bars represent SEM. ~ $p = .058$.

340x217mm (144 x 144 DPI)

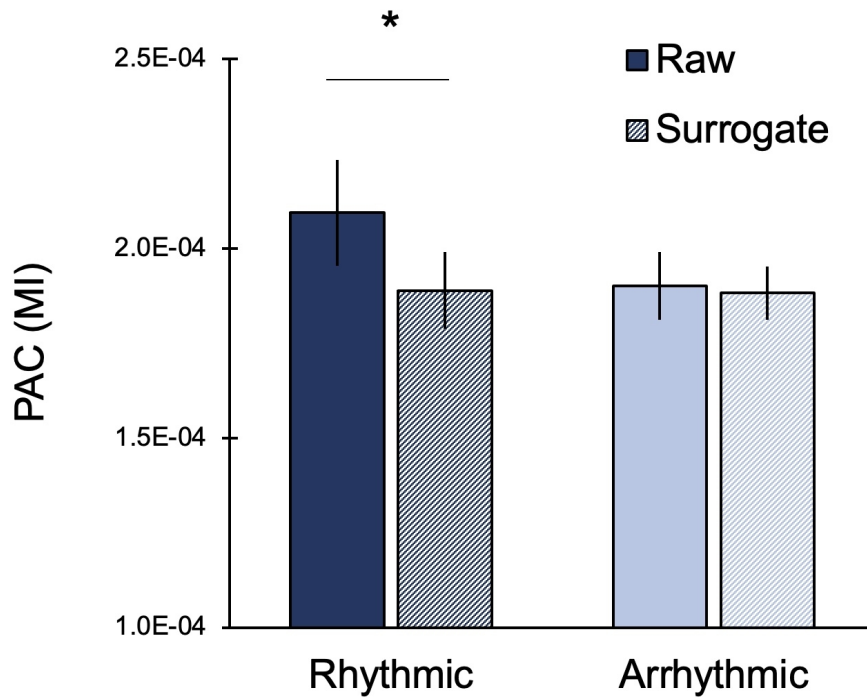


Figure 3. Significant phase-amplitude coupling (PAC; measured by MI) between the phase of entrained (1.67 Hz) oscillations and the amplitude of high-gamma (65-100 Hz) oscillations occurred in the rhythmic context only. Error bars represent SEM. * $p < .05$

255x196mm (144 x 144 DPI)

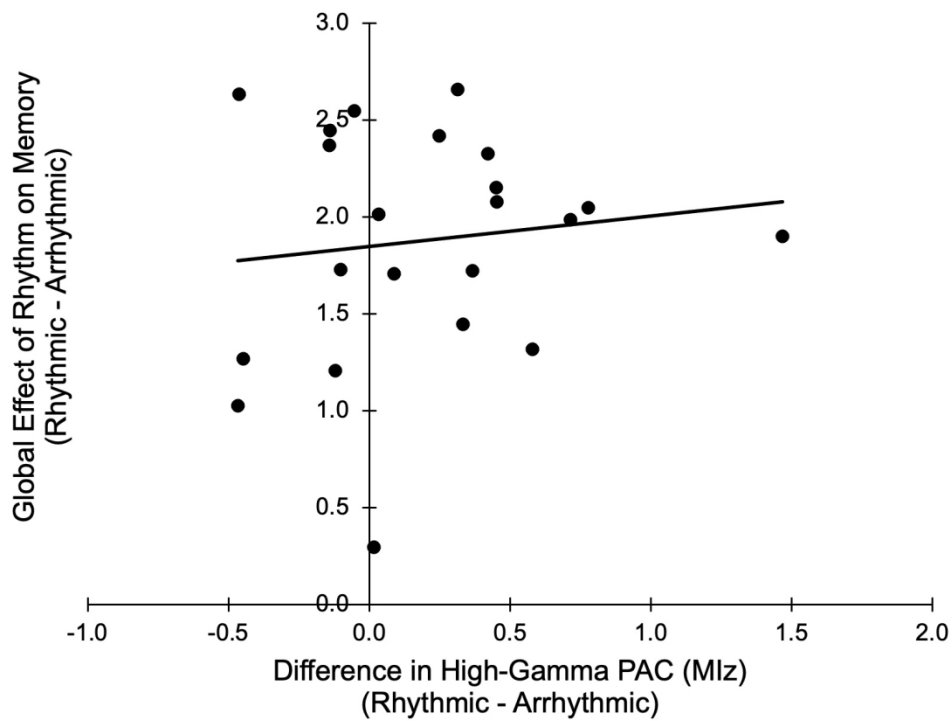


Figure 4. The difference in high-gamma phase amplitude coupling (PAC) between rhythmic and arrhythmic blocks showed a non-significant positive relationship with the global effect of rhythm on memory (d' rhythmic - d' arrhythmic).

297x222mm (144 x 144 DPI)

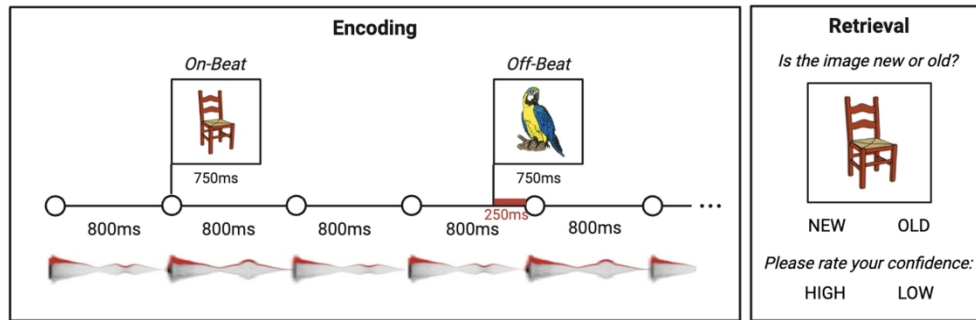


Figure 5. Experimental design for Study 2. Participants completed a single encoding (study) phase followed by a single retrieval (test) phase. During encoding, participants were shown a series of images in the context of music containing a steady 1.25 Hz beat. The beat timing is depicted using white circles above a schematic of the audio waveform of the music whose amplitude envelope is shown in red. Images were either presented synchronously (on-beat) or 250ms prior to the beat (off-beat). Each image remained on the screen for 750ms and participants were instructed to make a decision about whether the image was living or non-living. During retrieval, participants were given a self-paced memory tests where they identified if they had seen the image during the encoding task and their confidence (high, low) in their decision.

434x145mm (144 x 144 DPI)

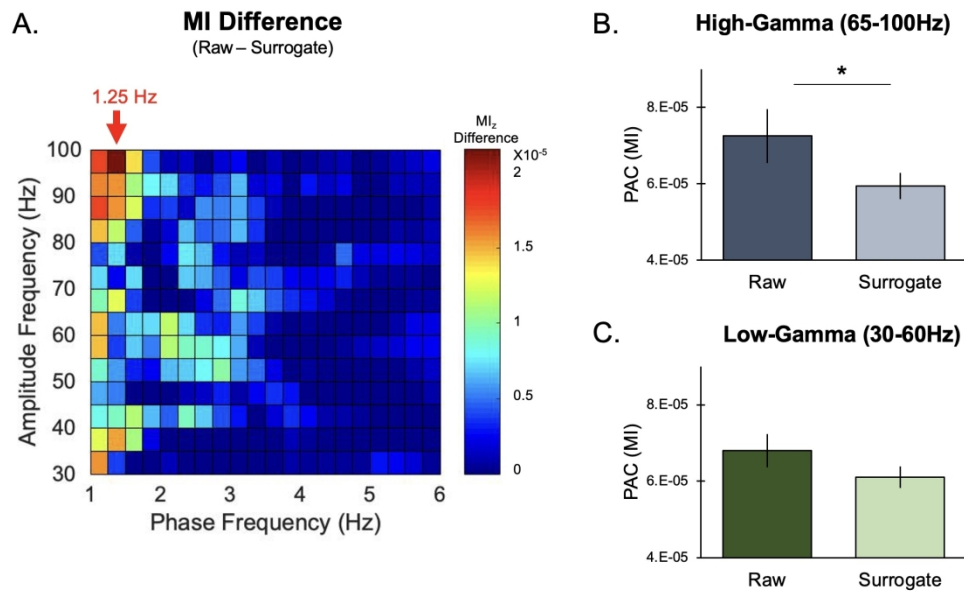


Figure 6. (A) Comodulogram displays the difference in phase-amplitude coupling (PAC; raw values - surrogate values) across the semantic decision task. Significant coupling (shown in warmer colors) is present between a range of lower (1.0-1.5 Hz) and higher (30-100 Hz) frequencies. However, peak coupling appears to occur between the entrained (1.25 Hz) oscillation and higher (80-100 Hz) frequencies. (B) Significant coupling occurred between the 1.25 Hz entrained oscillation and high-gamma (65-100 Hz) activity but, (C) not in the low-gamma range (30-60 Hz). Error bars represent SEM. * $p < .01$

376x226mm (144 x 144 DPI)

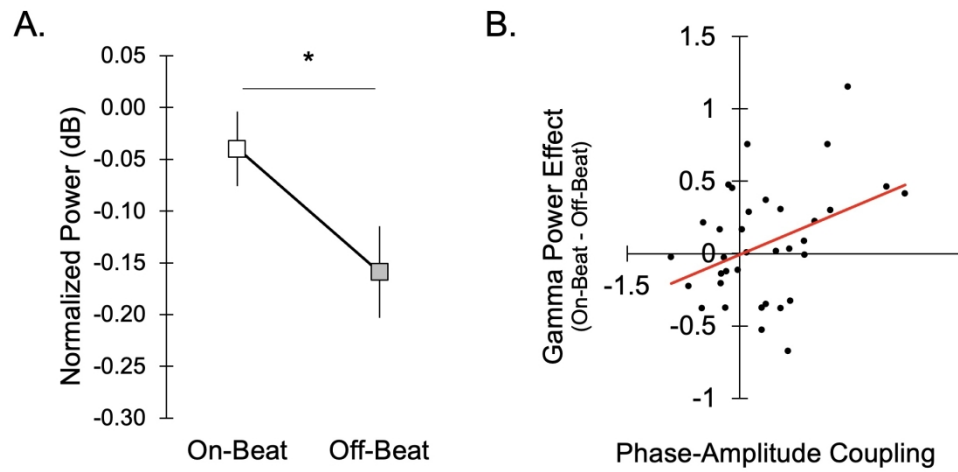


Figure 7. (A) Differences in gamma power (on-beat – off-beat). (B) At the time of stimulus presentation (-100:100ms), gamma power (30-100 Hz) is greater for on-beat compared with off-beat trials. (C) Importantly, in the high-gamma range, the strength of the coupling is related to the strength of the gamma power effects (on-beat > off-beat) in the high-gamma range. Error bars represent SEM. * $p < .05$

383x201mm (144 x 144 DPI)

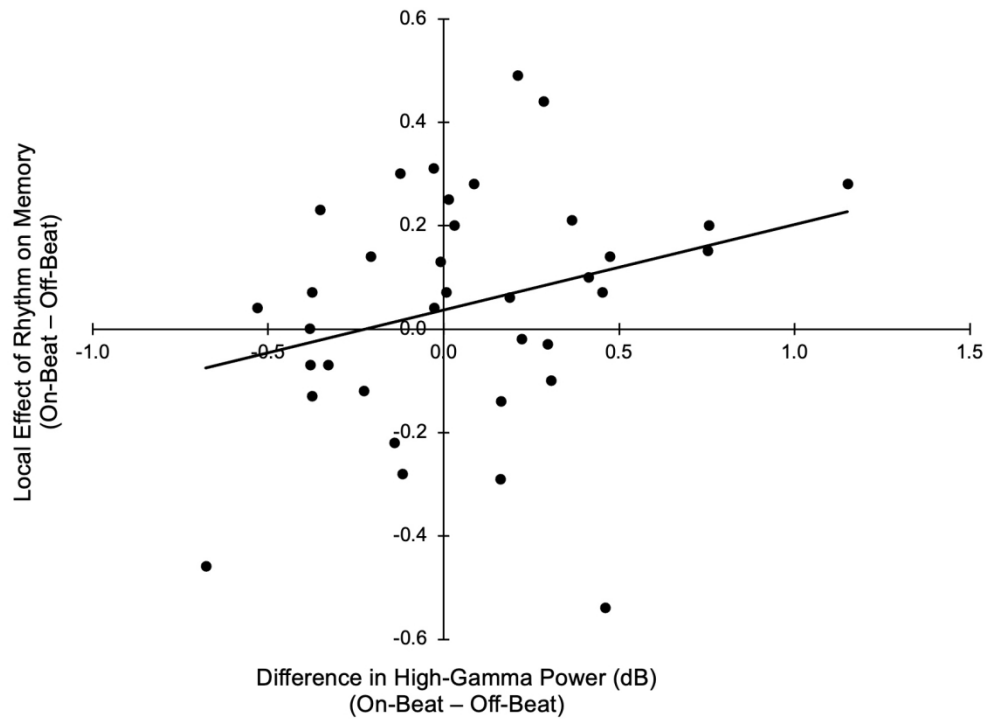


Figure 8. The difference in high-gamma phase power (dB) between on-beat and off-beat blocks showed is positively related with the local effect of rhythm on memory (d' on-beat - d' off-beat).

306x225mm (144 x 144 DPI)